NRL Report 6660

# A Subsatellite Area-of-View Circuit

R. J. Orsino and H. G. Talmadge, Jr.

*Applied Physics Branch*
*Applications Research Division*

April 30, 1968

NAVAL RESEARCH LABORATORY
Washington, D.C.

This document has been approved for public release and sale; its distribution is unlimited.

CONTENTS


| | |
|---|---|
| Abstract | ii |
| Problem Status | ii |
| Authorization | ii |
| INTRODUCTION | 1 |
| BASIC PRINCIPLES IN PAINTING THE CIRCLE ON THE DISPLAY | 1 |
| EQUATIONS FOR GENERATING CIRCLES ON A RECTANGULAR DISPLAY | 4 |
| EQUATIONS FOR GENERATING CIRCLES ON A POLAR DISPLAY | 9 |
| CIRCLE CIRCUIT BLOCK DIAGRAM | 11 |
| GAIN GATES FOR MERIDIAN CONVERGENCE | 13 |
| CONCLUSIONS | 15 |
| REFERENCES | 16 |
| APPENDIX A — Evaluation of $(X^2 + Y^2)^{1/2}$ | 17 |
| APPENDIX B — Meridian Convergence Correction Factor | 20 |
| APPENDIX C — Calculation of Numerical Values for Table 1 | 21 |
| APPENDIX D — Design Procedure for Circle Generator | 23 |
| APPENDIX E — Digital Control of Amplifier Gain | 31 |
| APPENDIX F — Stepwise Approximation to Meridian Convergence Contour | 37 |

## ABSTRACT

A subsatellite circle circuit is included in the NRL experimental satellite position prediction and display equipment (SPAD). This circuit paints, on the expanded display, a circle enclosing the area of view for a selected satellite. A combination of digital and analog techniques is used to generate a polygonal approximation to the ideal circle. Compensation for meridian convergence is provided, so that the resulting error is roughly equal to the degree to which an octagon approximates a circle. With simple circuit changes the polygon could have 12, 16, 20, or more sides.

The circle center is defined by the subsatellite position, and the SPAD prediction computer uses the satellite look-cone angle (say, that of a cloud-cover camera) and the satellite height to generate a circle radius in increments of 8 naut mi up to a maximum radius of 504 naut mi. This limit is determined by the practical requirement of displaying the circle only on the expanded display of limited area for any portion of the earth's surface. A duplicate circuit generates a circle about own ship's position.

The operational significance to be attached to the circles is of no concern in the present study. Rather, the circuit design approach, the design equations, and the circuit description at the block-diagram level are the important elements.

With suitable modification the circle circuit used for SPAD is applicable to any cathode-ray tube display having either electrostatic or magnetic deflection, providing the entire display surface is scanned by a method involving two orthogonal axes of deflection. The application is quite general and is not limited to the SPAD display of the earth's surface.


## PROBLEM STATUS

This is an interim report; work on the problem continues.

## AUTHORIZATION


NRL Problem Y01-01
Project XF 019-01-03-6168

Manuscript submitted October 13, 1967.

# A SUBSATELLITE AREA-OF-VIEW CIRCUIT

## INTRODUCTION

Included in the NRL satellite position prediction and display equipment (SPAD) (Fig. 1, also Refs. 1 through 7) is a circuit for generating and painting, on the expanded geographic display, an earth-surface area of view, or circle, of up to 1008 naut mi in diameter denoting, say, the area covered by a satellite-mounted cloud camera. This report is not concerned with the significance to be attached to the circle; it describes the analog-computer circuit devised to generate this circle and to present it on either a polar expanded display or a rectangular expanded display.

The circle circuit is essentially two circuits. A switchover occurs as the subsatellite position crosses the 75th parallel of latitude. On the polar expanded display the area outline closely resembles its true circular form, since little geometric distortion is involved. On the rectangular expanded display the circle must, in general, appear distorted, since the converging meridians here appear as parallel lines. Map scale factor and aspect ratio are such that, at the equator, a small circle on the display appears as an ellipse with the east-west axis shorter than the north-south axis. With correction for meridian convergence, the same small circle changes shape on the display such that the east-west axis exceeds the constant length of the north-south axis as the circle center moves away from the equator. The theoretical shape of the curve on this map projection is not exactly elliptical, of course, and for larger values of the radius the shape somewhat resembles a squat pear with the large end toward the pole.

As implemented, the circle circuit approximates the theoretical curves by straight line segments. Thus, the circle of the polar expanded display is approximated by an octagon, using a resistance-diode function generator developed in Great Britain. For the rectangular expanded display the basic circle circuit is electronically augmented to provide stepwise control of the longitudinal input voltage signals. This compensates for meridian convergence as the latitude sweep varies through its cycle for a given amount of off-centering in latitude.

## BASIC PRINCIPLES IN PAINTING THE CIRCLE ON THE DISPLAY

Comparatively simple basic principles and circuits are involved in painting a circle on a display surface while that surface is being scanned. These principles will be briefly presented before the situation is complicated by such practical matters as scale factors, display aspect ratio, computational approximations, stepwise compensation for meridian convergence, convexity of the display surface, deflection distortion, and generation and mixing of video pulses.

A representative scheme for painting a circle and map grids on a geographic display (as is done in SPAD) is shown in the block diagram of Fig. 2. The idealizing assumptions which apply to the preliminary discussion are (a) that the display surface is flat, (b) that the $X$ and $Y$ deflections are proportional to the $X$ and $Y$ voltages, (c) that there are no bandwidth limitations in the circuits, (d) that the $X$ and $Y$ deflection scale factors (in V/in.) are matched, and (e) that the electron beam is at the display center when $X = Y = 0$ V.

Fig. 1 - The laboratory installation of SPAD

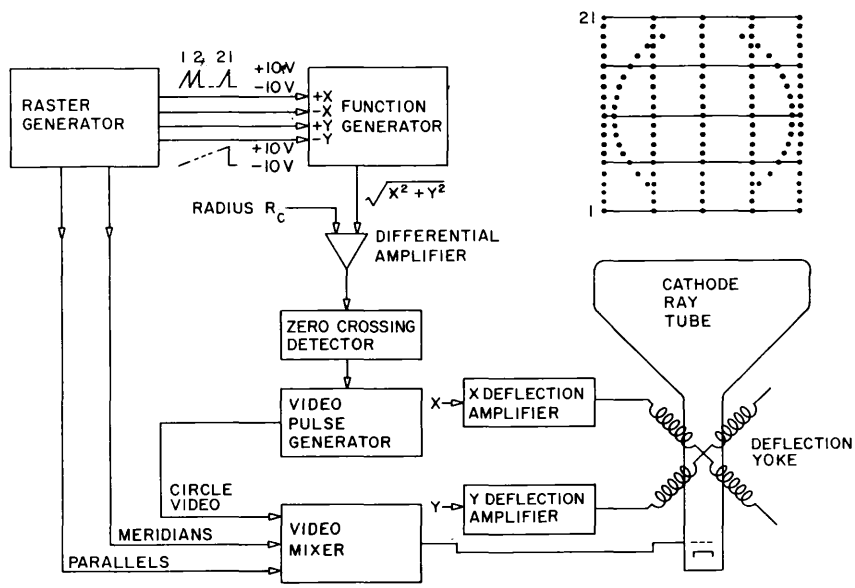


Fig. 2 - Generating the circle and map grids on an idealized display

The illustrative 21-line TV raster has a 1:1 aspect ratio, and the raster generator also generates meridian pulses and parallel gates, which, as video signals, suitably brighten the raster lines to produce the orthogonal map grid lines shown in the figure.

During each raster frame, circle video pulses are generated as follows. First, a function generator accepts push-pull sweep voltages, as shown, to generate a voltage denoted by $(X^2 + Y^2)^{1/2}$. In this instance the voltage is proportional to the radial distance from the display center to the scanning electron beam at any moment during each raster line. A differential amplifier compares this voltage with the circle radius voltage $R_c$. Each time they are equal the amplifier output voltage passes through zero, and a video pulse is generated. The equation

$$R_c = (X^2 + Y^2)^{1/2}$$

represents a circle of radius $R_c$ centered on the display. Consequently, a circle video pulse is painted on the display each time a raster line crosses the circle. The aggregate of circle video pulses then forms a dotted-line representation of a circle on the display.

This method of generating and painting a circle requires a rectangular-coordinate scheme for scanning the entire display surface during the frame interval in which the circle video pulses are generated. The function generator responds to the instantaneous values of $X$ and $Y$ and thus works equally well with either the TV raster of the rectangular expanded display or the radial scan of the polar expanded display. In fact, the circuit operates independently of the type of scan, providing the $X$ and $Y$ deflection voltages are based on orthogonal axes. While magnetic deflection of the scanning electron beam is indicated in the figure, electrostatic deflection is equally applicable.

Variations in this method of circle generation are possible. By suitably altering the inputs to the function generator, one can move the circle center to correspond to newly computed satellite positions. Likewise, the radius $R_c$ can be changed by the computer. When the voltages applied to the function generator are suitably scaled, the circle can

appear as an ellipse with its major axis either vertical or horizontal. Furthermore, a variation in this caling can produce various distortions in the shape of the circle as it appears on the display. All these variations are included in the design of the circle circuit described in this report.

## EQUATIONS FOR GENERATING CIRCLES ON A RECTANGULAR DISPLAY

Typical circles, as they appear on the rectangular expanded display, are shown in Figs. 3 and 4. Both figures represent an area 20 degrees in latitude by 30 degrees in longitude as a rectangle having a 3:4 aspect ratio, and both are selected portions of the modified cylindrical equal-spaced map projection described in Ref. 8. Near the equator (Fig. 3) the circle is approximated by an octagon, as discussed in Appendix A. When the satellite approaches 75° north latitude (Fig. 4), it is apparent how "stretching" the circle horizontally or longitudinally is accomplished in a stepwise fashion to approximate the desired smooth pear-shaped outline. The meridian-convergence correction factor which provides the theoretical basis for this stretching is derived in Appendix B.

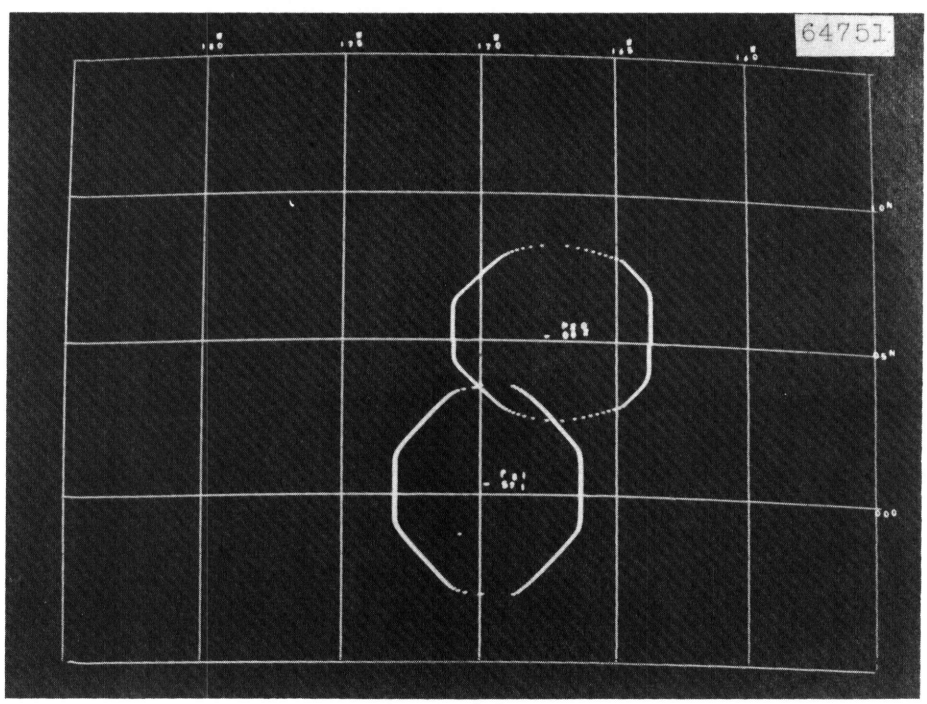


Fig. 3 - The rectangular expanded display with own ship, selected satellite, and areas of view near the equator. The selected satellite (lower position) also shows the vector dot.

Certain scale factors are calculated in Appendix C and are summarized in Table 1. These factors are used in Appendix D for deriving design equations for the circle circuit used with the rectangular expanded displays and the polar expanded displays. In Appendix E it is shown how the voltage gain of the horizontal (longitude) amplifier can be digitally controlled to provide a stepwise approximation to the correction for meridian convergence.

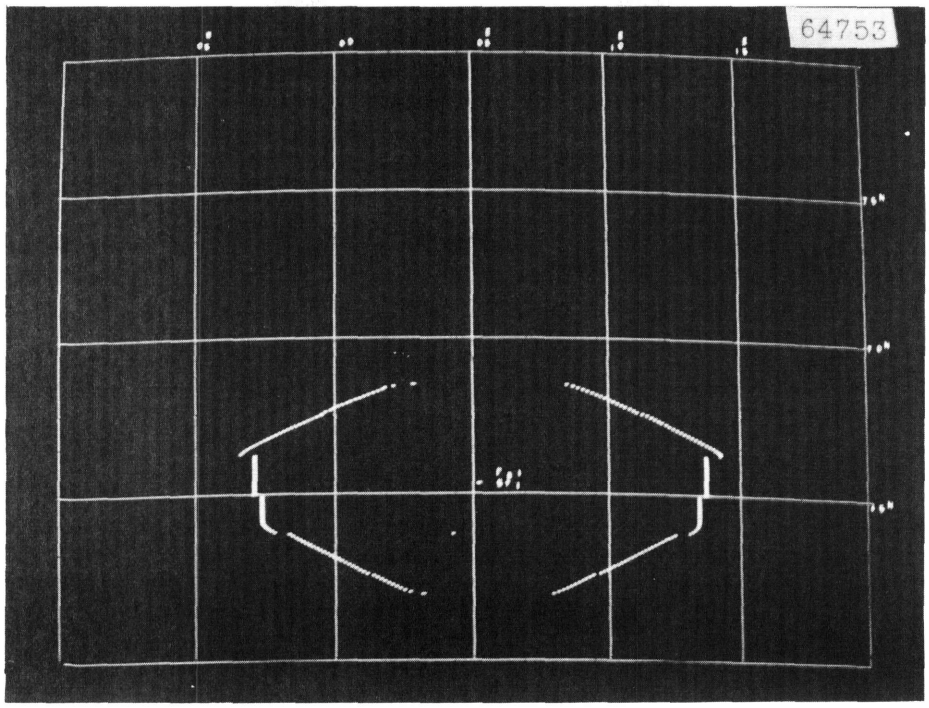


Fig. 4 - The approximation to a circle compensated for meridian convergence

A simplified block diagram for generating circle video for the rectangular expanded display is shown in Fig. 5. (With a suitable change in amplifier gain the same diagram applies to the polar display.) This diagram will be used for developing mathematical relationships, and it differs from the final circuit configuration in a few details.

The circuit action may be qualitatively described as follows: At a given instant the voltage $e_o$ from the function generator must be proportional to the distance in miles from the subsatellite position, denoted by dc voltages $T_v$ and $T_h$, to that point on the map presently scanned by the raster sweep voltages $V_s$ and $H_s$. The voltage $e_o$ is compared with the circle radius voltage $T_c$ to cause the comparator (Schmitt trigger) to change state whenever $e_o$ and $T_c$ are matched in mileage. In general, there will be two such transitions each time a raster line crosses the area-of-view circle having radius $T_c$. One transition will cause a one-shot multivibrator to generate a positive video pulse, as shown. Following a polarity inversion, the other transition will cause a second one-shot multivibrator to generate a similar video pulse. Both video pulses pass through a non-additive mixer circuit (a NOR circuit) which inverts the pulse polarity to provide the desired negative video pulses. It is these pulses which appear on the display as a suitable approximation to the desired circle.

The operation of the circuit in Fig. 5 will now be described with reference to a circle of radius $R_c$ having its center at the point $h, v$. For a rectangular Cartesian coordinate system with axes $H$, $V$, this circle is represented by

$$R_c^2 = (H-h)^2 + (V-v)^2 , \tag{1}$$

where $h$, $H$, $v$, $V$, and $R_c$ are defined in Table 1. During the raster period the distance $r$ from the circle center to any point in the $H$-$V$ plane is evidently

Table 1
Symbols and Definitions Relevant to the Expanded Display

| Symbol* | Definition |
|---|---|
| $h$ | Horizontal coordinate for the circle center, measured in naut mi from the left display boundary |
| $H$ | Horizontal coordinate for the instantaneous sweep position, measured in naut mi from the left display boundary |
| $v$ | Vertical coordinate for the circle center, measured in naut mi from the lower display boundary |
| $V$ | Vertical coordinate for the instantaneous sweep position, measured in naut mi from the lower display boundary |
| $R_c$ | Circle radius in naut mi |
| $T_h$ | Analog voltage denoting the horizontal coordinate of the circle center |
| $H_s$ | Horizontal sweep voltage for the display raster |
| $T_v$ | Analog voltage denoting the vertical coordinate of the circle center |
| $V_s$ | Vertical sweep voltage for the display raster |
| $T_c$ | Analog voltage representing the circle radius |
| $e_x$ | Input voltage for the horizontal amplifier |
| $X$ | Output voltage for the horizontal amplifier |
| $e_y$ | Input voltage for the vertical amplifier |
| $Y$ | Output voltage for the vertical amplifier |
| $G_y$ | Voltage amplification for the vertical amplifier |
| $G_x$ | Voltage amplification for the horizontal amplifier |
| $K_\phi$ | Meridian convergence correction factor (does not apply to the polar display) |
| $K_v$ | Scale factor for the vertical coordinate of the circle center (naut mi/V) |
| $K_h$ | Scale factor for the horizontal coordinate of the circle center (naut mi/V) |
| $K_V$ | Scale factor for the vertical sweep (naut mi/V) |
| $K_H$ | Scale factor for the horizontal sweep (naut mi/V) |
| $K_R$ | Scale factor for the circle radius (naut mi/V) |

*The context will indicate whether the symbols apply to the polar expanded display or to the rectangular expanded display. When an ambiguity exists, the subscript $p$ will be used to indicate the polar mode.

$$r = [(H-h)^2 + (V-v)^2]^{1/2}. \tag{2}$$

These two results will be shown to be relevant to Fig. 5. It will first be demonstrated that $r$, the distance in nautical miles from the circle center, can be interpreted in terms of voltage $e_o$ from the function generator in Fig. 5, where

$$e_o = K(X^2 + Y^2)^{1/2} \tag{3}$$

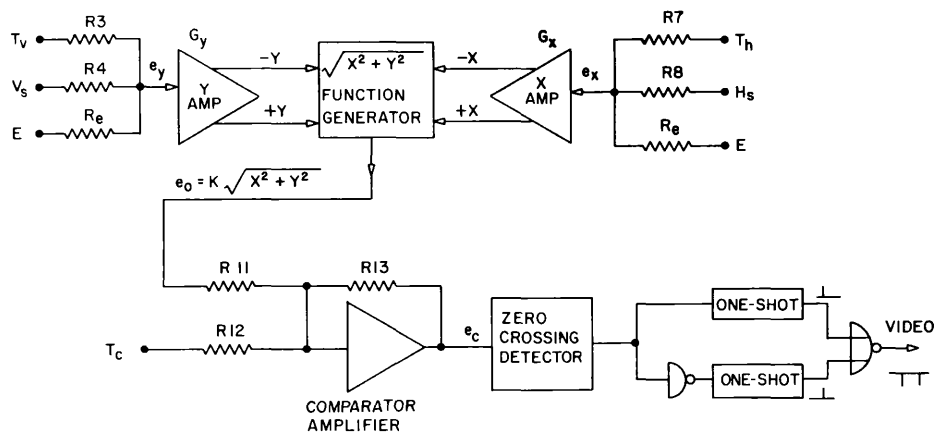


NOTE: R 11 is part of the function generator

Fig. 5 - A simplified circuit for generating circle video

and $K$ is a voltage attenuation constant characteristic of the function generator, as described in Appendix A. Then, to provide circle video pulses at the appropriate times during the raster, the circuit design relationship necessary for detecting the equality $r = R_c$ will be found.

In Appendix D it is shown how the amplifiers having voltage gains $G_y$ and $G_x/K_\phi$, along with their input resistor networks, produce the voltages $X$ and $Y$ given by

$$Y = \frac{R_e R_3}{K_V(R_e R_4 + R_e R_3 + R_3 R_4)} G_y (V - v) \tag{4}$$

and

$$X = \frac{R_e R_7}{K_H(R_e R_8 + R_e R_7 + R_7 R_8)} \frac{G_x}{K_\phi}(H - h) . \tag{5}$$

While $(V - v)$ and $(H - h)$ are expressed in nautical miles, the implied subtraction in each case is effected by summing two voltages having opposite polarities. Bias voltage $E$ of Fig. 5 serves to introduce an offset current via summing resistor $R_e$ so as to compensate for the dc component in the other input voltages. In Appendix D this is shown to be necessary in order to interpret the voltages $X$ and $Y$ in terms of nautical miles of deflection. Note that the meridian convergence factor $K_\phi$ has been included in Eq. (5), as discussed in Appendix B.

Let the coefficients of $(V - v)$ and $(H - h)$ be equated to establish the circuit design relationship needed to generate a circle:

$$\frac{R_e R_3 G_y}{K_V(R_e R_3 + R_e R_4 + R_3 R_4)} = \frac{R_e R_7 G_x}{K_\phi K_H(R_e R_7 + R_e R_8 + R_7 R_8)} . \tag{6}$$

This design constraint permits Eq. (3) to be rewritten in terms of Eqs. (4), (5), and (6) to obtain

$$e_o = \frac{K R_e R_3 G_y}{K_V(R_e R_3 + R_e R_4 + R_3 R_4)} [(H - h)^2 + (V - v)^2]^{1/2} \tag{7}$$

and, finally,

$$\frac{e_o K_V (R_e R_3 + R_e R_4 + R_3 R_4)}{K R_e R_3 G_y} = [(H-h)^2 + (V-v)^2]^{1/2}. \tag{8}$$

Now, from Eqs. (2) and (8), we can write

$$r = \frac{e_o K_V (R_e R_3 + R_e R_4 + R_3 R_4)}{K R_e R_3 G_y} . \tag{9}$$

This equation reveals that the function-generator output voltage $e_o$ can be interpreted in terms of $r$, the distance in nautical miles from $(h, v)$ the circle center to $(H, V)$ the point on the map being instantaneously scanned by the raster.

As has been stated, voltage $e_o$ is compared with a constant voltage representing the desired radius $R_c$. Thus, after considering the weighting factors, whenever $r$ equals $R_c$ the corresponding values of $H$ and $V$ and their associated sweep voltages $H_s$ and $V_s$ represent a point on the desired circle. Since the circle voltage $e_o$ and the circle radius voltage $T_c$ have opposite polarities, they are effectively subtracted by the summing resistors $R_{11}$ and $R_{12}$ of Fig. 5 and are amplified to provide a comparison voltage $e_c$. Assuming that the input junction to the comparator amplifier is at virtual ground, the nodal equation for this circuit can be written

$$\frac{e_c}{R_{13}} + \frac{e_o}{R_{11}} + \frac{T_c}{R_{12}} = 0. \tag{10}$$

From Table 1 and Appendix C we find that the circle radius is

$$R_c = -K_R T_c ; \tag{11}$$

therefore,

$$T_c = -\frac{R_c}{K_R} . \tag{12}$$

Here the minus sign merely indicates that, as SPAD was designed, a negative voltage $T_c$ represents a positive distance $R_c$. By convention, the scale factor $K_R$ is considered positive.

Substituting Eqs. (7) and (12) into Eq. (10) and rearranging, we obtain

$$e_c = -\frac{K R_e R_3 R_{13} G_y}{R_{11} K_V (R_e R_3 + R_e R_4 + R_3 R_4)} [(H-h)^2 + (V-v)^2]^{1/2} + \frac{R_{13}}{R_{12}} \frac{R_c}{K_R} . \tag{13}$$

To provide appropriate video pulses the zero-crossing detector must change state whenever the raster crosses the circle. Therefore, the comparison voltage $e_c$ must pass through zero volts whenever $r$ equals $R_c$. These conditions will be satisfied in Eq. (13), provided

$$\frac{K R_e R_3 R_{13} G_y}{R_{11} K_V (R_e R_3 + R_e R_4 + R_3 R_4)} = \frac{R_{13}}{R_{12} K_R} .$$

Dividing by $R_{13}$ yields

$$\frac{KR_eR_3G_y}{R_{11}K_V(R_eR_3 + R_eR_4 + R_3R_4)} = \frac{1}{R_{12}K_R}, \tag{14}$$

which provides the final design relationship. While resistor $R_{13}$ does not appear in this equation, its value is chosen to make the hysteresis effects of the zero-crossing detector (Schmitt trigger) negligible. This hysteresis is the voltage interval between the upper and the lower triggering levels of the circuit.

For brevity in the text, the theoretical treatment has intentionally by-passed many intermediate steps required for a practical design. However, a few comments can be offered relating this theory to the practical design procedure followed in Appendix D.

To compensate for meridian convergence, it is necessary that

$$G_x = 1.5\ G_y \cos \phi, \tag{15}$$

as shown in Appendix D. That is, the voltage amplification in the longitudinal coordinate for a given raster line must vary directly with the cosine of the latitude for that raster line on the rectangular expanded display, up to a maximum latitude of nearly 80°. In the final circuit a stepwise approximation to the cosine function is achieved by using six electronic clamps to control the gain $G_x$ digitally. The resulting quantization errors roughly equal the degree to which an octagon approximates a circle, as shown in Appendix F, Table F1.

While resistor $R_{11}$ is shown external to the function generator of Fig. 5, in practice it will be an integral part of that generator. The value of $R_{11}$ is not limited by the generator theory. Various circuit configurations are available which provide better accuracies with relatively simple circuits, as discussed in Appendix A.

## EQUATIONS FOR GENERATING CIRCLES ON A POLAR DISPLAY

As the circle center crosses the 75th parallel to approach either pole, the display automatically changes from rectangular to polar coordinates. In response to a signal generated at the position prediction computer, mechanical relays in the SPAD display formatter are energized to cause the following circuit changes: (a) the vertical and horizontal sawtooth sweep generators now generate voltages $V_{ps}$ and $H_{ps}$ for the polar raster in place of voltages $V_s$ and $H_s$ for the TV raster of the rectangular expanded display, (b) compensation for meridian convergence is removed, and (c) the gain of the $X$ and $Y$ amplifiers is switched to new values.

With the rectangular-mode input signals of the circuit shown in Fig. 5 replaced by their polar-mode counterparts, the analysis in Appendix D indicates it is merely necessary that

$$G_{px} = G_{py} = 2G_y\,. \tag{16}$$

That is, the voltage amplifications of the $X$ and $Y$ amplifiers during the polar mode of operation are twice that of the $Y$ amplifier when a rectangular display is painted. The use of precision resistors, precision digital-to-analog decoders, and precise adjustment of sweep amplitudes and baselines permits Eq. (16) to be achieved with a minimum of switching. The only other calibration adjustments are part of the model ST-35 Schmitt trigger used as the zero-crossing detector (Fig. 6).

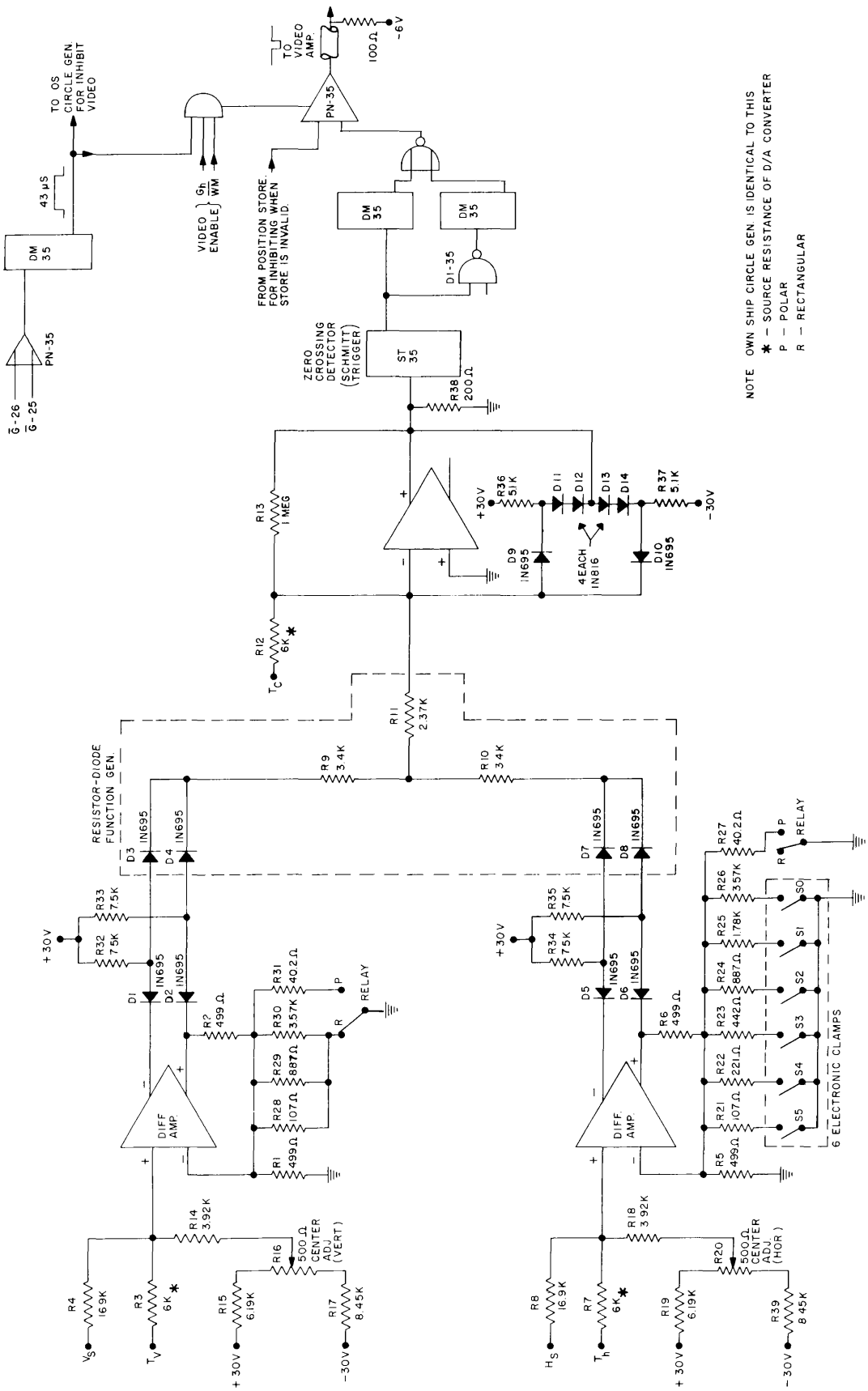


Fig. 6 - The satellite circle generator

A circle appears on the polar display as the octagon of Fig. 7. Here the grid lines represent a map projection of the polar region on a plane tangent at the pole with parallels of latitude forming equispaced concentric rings. Theoretically, there is circle distortion besides that resulting from the octagonal approximation. Thus, even if such minor effors as octagonal approximation, amplifier drift, bandwidth limitation, resistor tolerance, sweep nonlinearity, wandering sweep baseline, nonsinusoidal sweep envelope, digital quantization, and decoding errors were entirely eliminated, the resultant curve could not exactly represent the subsatellite view area, even though it was studied with reference to the map grid lines to eliminate deflection distortions on the viewing surface of the cathode-ray tube. The residual error is considered negligible and will not be evaluated until a firm requirement for the circle has been established.

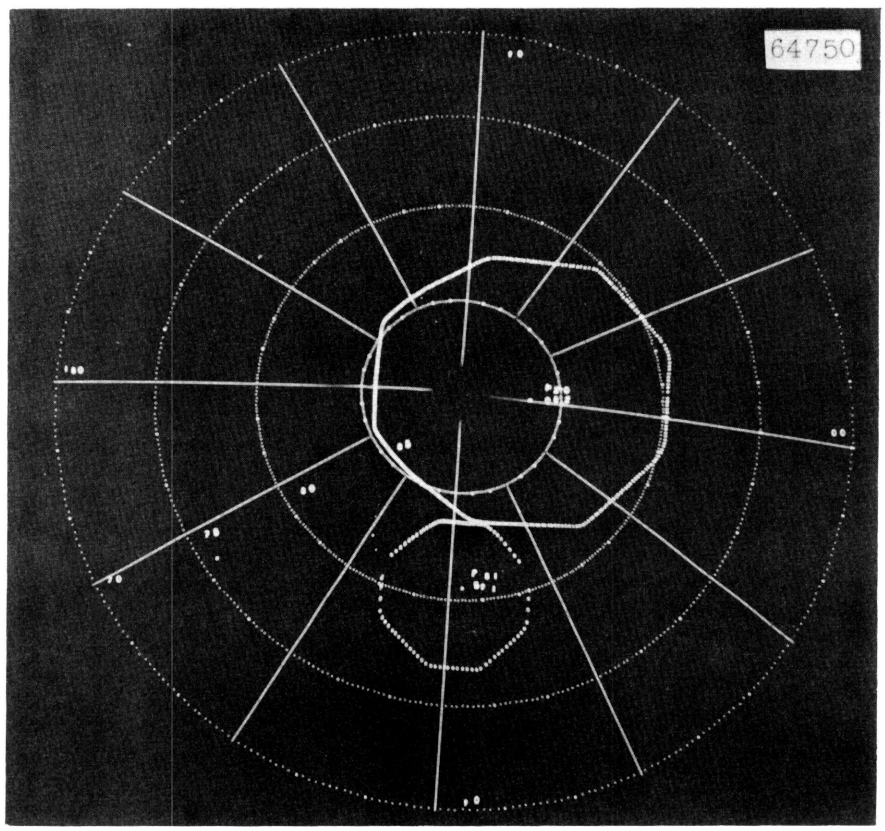


Fig. 7 - The polar expanded display with own ship, selected satellite, and areas of view

## CIRCLE CIRCUIT BLOCK DIAGRAM

The general approach for generating circle video pulses as a raster scans the display surface has been described in detail with reference to a simplified block diagram. Further details of how this concept is implemented in SPAD will now be presented in two steps. First, the analog circuits for generating circle video pulses are described together with the associated gating logic for inhibiting this video. These circuits include switches which control the voltage gain in the analog amplifiers. A separate discussion includes the digital circuits for the gain gates which operate these switches to vary the voltage gain in discrete jumps allowing compensation for meridian convergence.

Analog circuits for generating circle video are shown in Fig. 6, a combination circuit diagram and block diagram. For each coordinate there is a resistor mixing circuit which, in effect, subtracts the circle center voltage from the instantaneous deflection voltage. Another resistor adds a center adjustment voltage to compensate for the dc component in the circle center voltage for each coordinate. Thus, resistors $R_{14}$ and $R_{18}$ of Fig. 6 correspond to $R_e$ of Fig. 5, with the voltages corresponding to $E$ coming from CENTER ADJ, calibration controls $R_{16}$ and $R_{20}$ for the vertical and horizontal coordinates, respectively. The two circle center voltages $T_v$ and $T_h$ come from digital-to-analog decoders which have a source resistance of 6 kilohms, shown as $R_3$ and $R_7$, respectively.

A differential amplifier for each coordinate is shown as generating push-pull output voltages, with an attenuated portion of one output providing negative feedback to control the voltage gain. For each amplifier a relay switching section has positions denoted $R$ and $P$ to establish the gain for the rectangular and polar rasters, respectively. Each amplifier accepts the output of its respective resistor mixing circuit to generate a useful output voltage varying between -10 V and +10 V. The amplifier is designed to recover from an overload in less than a microsecond.

The voltage gain of the horizontal differential amplifier is also controlled by the six bidirectional electronic clamps represented, for simplicity, as the switches $S_0$ through $S_5$ in Fig. 6. For the polar expanded display these switches are held fixed in some suitable state. For the rectangular expanded display, however, when the relay arms are in the "$R$" position, the state of these six switches is altered during certain horizontal-sweep dead times of each raster period. The switching method will be described later. Design equations for predicting the resulting voltage gain are derived in Appendix E.

In practice, the horizontal and vertical amplifiers with push-pull output voltages consist of two operational amplifiers with negative feedback. The amplifiers are cascaded, with a positive-gain amplifier providing the "plus" output and driving an inverting amplifier which provides the "minus" output.

Each push-pull output signal passes through a simple resistance-diode network intended to compensate for the diode voltage drop in the following resistance-diode function generator. This function generator, described in Appendix A, generates, across load resistor $R_{11}$, a voltage proportional to the root-mean-square value of the horizontal and vertical input voltages.

The voltage across $R_{11}$ may also be considered to represent the distance from the circle center to the point on the map being scanned by the electron beam of the cathode-ray tube. This voltage is compared with the circle radius voltage $T_c$ generated in a digital decoder having an output resistance $R_{12}$ of 6 kilohms. The summing junction of $R_{11}$ and $R_{12}$ operates at ground potential, since this junction is at the virtual ground point of an operational amplifier. The output voltage of this amplifier passes through zero whenever the electron beam scans across the periphery of the circle. At other times the nonlinear feedback network of this operational amplifier clamps the output excursions to within a fraction of a volt from ground. The following Schmitt trigger generates a digital transition whenever the comparator amplifier output voltage passes through zero. Since the Schmitt trigger circuit has a certain hysteresis effect (i.e., the triggering level is a function of the direction of the signal excursion), the operational amplifier is needed to reduce the effect of hysteresis on the circle shape.

Standard digital-logic circuits operate on the output transitions of the model ST-35 Schmitt trigger to generate a narrow video pulse each time the electron beam scans across the circle boundary. These video pulses are combined in a nonadditive mixer (a NOR circuit) and then passed through a model PN-35 power amplifier which drives the coaxial video line to the display console.

Certain video-inhibit and video-enable gates are also applied to the input of the PN-35 power amplifier to permit only valid circle video to be displayed. For instance, the horizontal sweep gate $G_h$ passes pulses during a sweep interval and inhibits those pulses generated during the sweep flyback time. The negation of the world map gate, denoted $\overline{WM}$, enables circle video whenever an expanded display is presented.

Circle video must also be inhibited when an invalid position is held in the circle center store. Suppose the display were expanded about own ship at the operator's discretion, and that the TN satellite for which a circle is nominally desired happens to be at, say, the antipode. Since a valid position cannot now be placed in the satellite circle center store $TN_x$, the prediction computer forces the two most significant bits to the logical ONE level to denote this fact. A NAND circuit (not shown) senses these two bits and generates a video-inhibit gate which is also applied to the PN-35 power amplifier. This gate inhibits satellite circle video until the satellite enters the area covered by the expanded display.

Circle video for both own ship and the satellite is inhibited whenever the circle center stores and the circle radius stores for either own ship or the satellite are being updated. The address gates G26 and G25, which are, in turn, rendered true during the updating of the associated stores, have their complements $\overline{G}26$ and $\overline{G}25$ combined in the OR amplifier model PN-35. Thus, the leading edge of either gate causes the one-shot multivibrator model DM-35 to generate a 43-$\mu$sec gate which inhibits both the satellite circle video and the own ship circle video. This inhibit gate is somewhat longer than either address gate to permit all circuits to settle before circle video is again painted. (While this circuit configuration is somewhat unconventional, it performs satisfactorily while using digital module sections which would be otherwise unassigned.) A similar description applies to the own ship circle generator which is now shown.

## GAIN GATES FOR MERIDIAN CONVERGENCE

The six bidirectional electronic clamps, shown as switches $S_0$ through $S_5$ in Fig. 6, have their states altered during certain horizontal sweep retrace times depending on the latitudinal off-centering of the expanded display and the state of a raster line counter. The objective is to vary the voltage gain of the longitudinal amplifier in the circle circuit in a stepwise fashion so that it approximately conforms to the meridian-convergence correction factor discussed in Appendix B. Since SPAD represents only one use of a concept having broad applications, only enough details will be provided to suggest how the circle circuit can be used.

The counter states, and the corresponding states of the bidirectional clamps, are shown in Table 2. These states cause the gain to approximate a cosine function (Fig. F1), as shown in Appendix E. The clamps change state only every 90 raster lines near the equator, where the cosine function changes slowly. Near the poles, where the cosine function changes more rapidly, the clamps change state every 23 raster lines, or every 1.26 degrees in latitude, for the 361-line raster.

Consider the operation for the southernmost rectangular expanded display. The SPAD computer designates the amount of off-centering by gating the off-center word $\phi_c$ = 00000 into the map grid counter. From left to right, these binary digits are known as the $2^4$, $2^3$, $2^2$, $2^1$, and $2^0$ bits, and this initial value denotes that the initial raster line at the bottom of the display represents 80 degrees south latitude. At every 90 lines of the noninterlaced raster the $\phi_c$ counter is incremented one count, and map grids are painted at 5-degree latitude intervals, always proceeding from south to north. Beginning with each map grid line, a two-stage counter having bits denoted $2^{-1}$ and $2^{-2}$ is reset and then incremented each 23 raster lines. Thus, each five-degree latitude interval is divided into four approximately equal intervals in order to control the clamp states.

Table 2
Counter States Controlling Bidirectional Clamps

| Map Grid | $2^4$ | | | | $2^0$ | $2^{-1}$ | $2^{-2}$ | OD Output Line | BDC* 0 | 1 | 2 | 3 | 4 | 5 |
|---|---|---|---|---|---|---|---|---|---|---|---|---|---|---|
| | $\phi_c$ | | | | | ÷ 4 | | | | | | | | |
| 80 S | 0 | 0 | 0 | 0 | 0 | 0 | 0 | 1-0 | | | | | | |
| | 0 | 0 | 0 | 0 | 0 | 0 | 1 | 1-1 | | x† | | | | |
| | 0 | 0 | 0 | 0 | 0 | 1 | 0 | 1-2 | x | x | | | | |
| | 0 | 0 | 0 | 0 | 0 | 1 | 1 | 1-3 | x | | x | | | |
| 75 S | 0 | 0 | 0 | 0 | 1 | 0 | 0 | 1-4 | x | x | x | | | |
| | 0 | 0 | 0 | 0 | 1 | 0 | 1 | 1-5 | | | | x | | |
| | 0 | 0 | 0 | 0 | 1 | 1 | 0 | 1-6 | | x | | x | | |
| | 0 | 0 | 0 | 0 | 1 | 1 | 1 | 1-7 | x | x | | x | | |
| 70 S | 0 | 0 | 0 | 1 | 0 | 0 | 0 | 2-0 | x | | x | x | | |
| | 0 | 0 | 0 | 1 | 0 | 0 | 1 | 2-1 | x | x | x | x | | |
| | 0 | 0 | 0 | 1 | 0 | 1 | 0 | 2-2 | | | | | x | |
| | 0 | 0 | 0 | 1 | 0 | 1 | 1 | 2-3 | | x | | | x | |
| 65 S | 0 | 0 | 0 | 1 | 1 | 0 | 0 | 2-4 | x | x | | | x | |
| | 0 | 0 | 0 | 1 | 1 | 0 | 1 | 2-5 | x | | x | | x | |
| | 0 | 0 | 0 | 1 | 1 | 1 | 0 | 2-6 | | x | x | | x | |
| | 0 | 0 | 0 | 1 | 1 | 1 | 1 | 2-7 | | | | x | x | |
| 60 S | 0 | 0 | 1 | 0 | 0 | 0 | | 3-0 | | x | | x | x | |
| | 0 | 0 | 1 | 0 | 0 | 1 | | 3-1 | x | | x | x | x | |
| 55 S | 0 | 0 | 1 | 0 | 1 | 0 | | 3-2 | x | x | x | x | x | |
| | 0 | 0 | 1 | 0 | 1 | 1 | | 3-3 | | x | | | | x |
| 50 S | 0 | 0 | 1 | 1 | 0 | 0 | | 3-4 | x | | x | | | x |
| | 0 | 0 | 1 | 1 | 0 | 1 | | 3-5 | x | x | x | | | x |
| 45 S | 0 | 0 | 1 | 1 | 1 | 0 | | 3-6 | x | | | x | | x |
| | 0 | 0 | 1 | 1 | 1 | 1 | | 3-7 | | | x | x | | x |
| 40 S | 0 | 1 | 0 | 0 | 0 | | | 4-0 | x | x | x | x | | x |
| 35 S | 0 | 1 | 0 | 0 | 1 | | | 4-1 | x | x | | | x | x |
| 30 S | 0 | 1 | 0 | 1 | 0 | | | 4-2 | | x | x | | x | x |
| 25 S | 0 | 1 | 0 | 1 | 1 | | | 4-3 | x | | | x | x | x |
| 20 S | 0 | 1 | 1 | 0 | 0 | | | 4-4 | x | x | | x | x | x |
| 15 S | 0 | 1 | 1 | 0 | 1 | | | 4-5 | x | | x | x | x | x |
| 10 S | 0 | 1 | 1 | 1 | 0 | | | 4-6 | | x | x | x | x | x |
| 05 S | 0 | 1 | 1 | 1 | 1 | | | 4-7 | x | x | x | x | x | x |

| Map Grid | $2^4$ | | | | $2^0$ | $2^{-1}$ | $2^{-2}$ | OD Output Line | BDC* 0 | 1 | 2 | 3 | 4 | 5 |
|---|---|---|---|---|---|---|---|---|---|---|---|---|---|---|
| | $\phi_c$ | | | | | ÷ 4 | | | | | | | | |
| 00 | 1 | 0 | 0 | 0 | 0 | | | 4-7 | x | x | x | x | x | x |
| 05N | 1 | 0 | 0 | 0 | 1 | | | 4-6 | | x | x | x | x | x |
| 10N | 1 | 0 | 0 | 1 | 0 | | | 4-5 | x | | x | x | x | x |
| 15N | 1 | 0 | 0 | 1 | 1 | | | 4-4 | x | x | | x | x | x |
| 20N | 1 | 0 | 1 | 0 | 0 | | | 4-3 | x | | | x | x | x |
| 25N | 1 | 0 | 1 | 0 | 1 | | | 4-2 | | x | x | | x | x |
| 30N | 1 | 0 | 1 | 1 | 0 | | | 4-1 | x | x | | | x | x |
| 35N | 1 | 0 | 1 | 1 | 1 | | | 4-0 | x | x | x | x | | x |
| 40N | 1 | 1 | 0 | 0 | 0 | 0 | | 3-7 | | | x | x | | x |
| | 1 | 1 | 0 | 0 | 0 | 1 | | 3-6 | x | | | x | | x |
| 45N | 1 | 1 | 0 | 0 | 1 | 0 | | 3-5 | x | x | x | | | x |
| | 1 | 1 | 0 | 0 | 1 | 1 | | 3-4 | x | | x | | | x |
| 50N | 1 | 1 | 0 | 1 | 0 | 0 | | 3-3 | | x | | | | x |
| | 1 | 1 | 0 | 1 | 0 | 1 | | 3-2 | x | x | x | x | x | |
| 55N | 1 | 1 | 0 | 1 | 1 | 0 | | 3-1 | x | | x | x | x | |
| | 1 | 1 | 0 | 1 | 1 | 1 | | 3-0 | | x | | x | x | |
| 60N | 1 | 1 | 1 | 0 | 0 | 0 | 0 | 2-7 | | | | x | x | |
| | 1 | 1 | 1 | 0 | 0 | 0 | 1 | 2-6 | | x | x | | x | |
| | 1 | 1 | 1 | 0 | 0 | 1 | 0 | 2-5 | x | | x | | x | |
| | 1 | 1 | 1 | 0 | 0 | 1 | 1 | 2-4 | x | x | | | x | |
| 65N | 1 | 1 | 1 | 0 | 1 | 0 | 0 | 2-3 | | x | | | x | |
| | 1 | 1 | 1 | 0 | 1 | 0 | 1 | 2-2 | | | | | x | |
| | 1 | 1 | 1 | 0 | 1 | 1 | 0 | 2-1 | x | x | x | x | | |
| | 1 | 1 | 1 | 0 | 1 | 1 | 1 | 2-0 | x | | x | x | | |
| 70N | 1 | 1 | 1 | 1 | 0 | 0 | 0 | 1-7 | x | x | | x | | |
| | 1 | 1 | 1 | 1 | 0 | 0 | 1 | 1-6 | | x | | x | | |
| | 1 | 1 | 1 | 1 | 0 | 1 | 0 | 1-5 | | | | x | | |
| | 1 | 1 | 1 | 1 | 0 | 1 | 1 | 1-4 | x | x | x | | | |
| 75N | 1 | 1 | 1 | 1 | 1 | 0 | 0 | 1-3 | x | | x | | | |
| | 1 | 1 | 1 | 1 | 1 | 0 | 1 | 1-2 | x | x | | | | |
| | 1 | 1 | 1 | 1 | 1 | 1 | 0 | 1-1 | | x | | | | |
| | 1 | 1 | 1 | 1 | 1 | 1 | 1 | 1-0 | | | | | | |

*Switches $S_0$ through $S_5$.

†A closed clamp is denoted by x.

Of the 64 possible states for the six clamps, only 32 are used to approximate the cosine function. Each of these states appears twice in Table 2 due to the symmetry with respect to the equator. That is, there are two counter states (bits $2^{-2}$ through $2^{4}$) for each clamp state listed in the table. One counter state represents a certain latitude interval north of the equator, and the other counter state represents (not exactly) the same latitude interval south of the equator. Now the state for the north interval can be converted to the state for the south interval simply by complementing each bit. This property, and the fact that certain of the $2^{-1}$ and $2^{-2}$ bits are not used to determine certain clamp states, makes it possible to use only four octal decoders (OD) to generate the 32 OD output lines denoted 1-0 through 4-7. These 32 lines comprise the gain gates which, through suitable connection to the six clamps in each circle circuit, serve to compensate for meridian convergence as further described in Appendix E. The clamp action is inhibited for both the polar display of Fig. 7 and the world map display, which is not shown.

## CONCLUSIONS

The foregoing method of generating and displaying a circle on a display during the raster scan interval has both advantages and disadvantages. An important advantage for the SPAD application is that comparatively little computer programming and computation time are required to generate the circle radius and the circle center information, as contrasted with that involved in generating many points on the periphery of the area of view. A simple (in its basic form) analog computer operates on this radius and the center information to generate video pulses which appear as a fine-textured dotted line. The polygonal approximation to a circle is believed to be adequate for most applications, including the present, and can readily and simply be increased from eight to 12, 16, 20, etc. sides.

However, from the aesthetic viewpoint, certain disadvantages appear. As a minor matter, circle texture on both the polar raster display (Fig. 7) and the TV raster display (Fig. 3) varies from fine to coarse along the periphery of the circle. Much more annoying, but still tolerable, are the gaps in the circle which appear when a side of the polygon falls upon a raster line. This will always be true for the top and bottom sides of an octagon (Fig. 3) painted by a TV raster. Fortunately, this limitation is readily removed by using a 12-sided or 20-sided figure for which no side falls upon a TV raster line. (In some instances, however, a side could fall upon a polar raster line and result in a gap. But the gap for a 20-sided polygon would be only 40 percent the size of a corresponding gap for an octagon.)

The simplicity inherent in the analog computer used in the circle circuit is somewhat overshadowed by the complexity of the digital circuitry used to compensate for meridian convergence in the SPAD application. Even greater complexity would be needed to add the one or more bidirectional clamps needed to make the discontinuities which provide this compensation in the circle of Fig. 4 less annoying.

The circle circuit implemented for SPAD adequately demonstrated the concept of displaying a satellite area-of-view circle. Since SPAD would be a research tool and not the final operational equipment, no attempt was made to measure or secure the ultimate performance in this circle circuit. Improvements in performance could be achieved.

The circle circuit has other possible applications whenever the display surface is scanned by any of the several rasters involving $X$ and $Y$ deflection components. Thus, the sweep voltages alone could be manipulated to generate a voltage proportional to the instantaneous deflection from the display center, and this voltage could be used in a dynamic-focus current-control circuit. Or, if this voltage were passed through the voltage comparator, the gate pulses from the Schmidt trigger could be used to blank the display whenever the beam was deflected just off the display screen of a round cathode-ray

tube. Small circles or ellipses could be painted anywhere on the display, provided the raster had adequate resolution to present a useful curve. The dimensions of the ellipse might, for instance, represent the measurement errors associated with a data point being plotted. In another application the gate pulse associated with a circle might be used to gate the video within the circle into another display for further analysis.

The circle circuit could also be adapted to generate an analog voltage proportional to the distance between any two points represented by two sets of $X$ and $Y$ potentials. Or, this analog voltage could be compared with some threshold value to cause the Schmidt trigger output to ring an alarm or otherwise alert the operator whenever any pair of points in a sequence rapidly selected by a digital computer were separated by a computed distance either less than or greater than some threshold value which may be determined by the computer.

In these suggested applications the computation speed is limited by the settling time of the analog amplifiers and the Schmidt trigger. Thus, the speed of the digital computer in selecting and presenting the input data may well be the limiting factor.

It may be said then that the circle circuit is reasonably satisfactory in the SPAD application. Furthermore, it has many possible applications, some of which have been listed to suggest its great versatility.

## REFERENCES

1. Kulikowski, E.F., "Proposed Study and Development of Earth Satellite Display Equipment," Enclosure (1) to NRL letter to the Bureau of Ships; 5110-39:EFK:eam Ser 5197, May 31, 1960

2. Hall, G.L., "Satellite Track Computation for Display Purposes," NRL Report 5652, Oct. 3, 1961

3. Talmadge, H.G., Jr., "An Orbit Computer for a Satellite Position Display," NRL Report 5624, July 31, 1961

4. Talmadge, H.G., Jr., "A Shipboard Satellite Position Display," NRL Report 5638, Aug. 7, 1961

5. Talmadge, H.G., Jr., and Orsino, R.J., "SPAD - A Satellite Position Prediction Display," published in the proceedings of the Third National Symposium on Information Display, sponsored by the Society for Information Display, San Diego, California, Feb. 1964

6. Talmadge, H.G., Jr., and Orsino, R.J., "Operation and Performance of the NRL Satellite Position Display," NRL Report 6219, Aug. 11, 1965

7. Orsino, R.J., and Boller, J.R., "SPAD Formatter—The Buffer Interface Between the Satellite Prediction Computer and the Display," NRL Report 6431, Oct. 11, 1966

8. Coast and Geodetic Survey, "Elements of Map Projection," Government Printing Office Special Publication 68, 5th Edition, Rev. 1944, p.33

## Appendix A

## EVALUATION OF $(X^2 + Y^2)^{1/2}$

Relatively simple resistance-diode function generators (Refs. A1 and A2) have been devised to generate a voltage proportional to the function $(X^2 + Y^2)^{1/2}$, where $X$ and $Y$ are input voltages. In all these generators (for ideal diodes) the output remains constant as the input follows the contour of a regular polygon (e.g., octagon, dodecagon, etc.), being symmetric to the $X$ and $Y$ axes.

The simplest circuit (with several variants) introduces equal plus and minus errors of about 4 percent. This error is acceptable here, since the corresponding octagon is a reasonable approximation to the desired circle. Furthermore, the correction for meridian convergence (see Appendix B), by acting in discrete jumps, introduces errors of about 5 percent as is further discussed in Appendix F.

### THE OCTAGON CIRCUIT

The basic circuit used in generating the area-of-view circle is shown in Fig. A1 with the appropriate design and performance information. This variant of the octagon circuit, although producing a relatively low output voltage, was chosen because this voltage is developed across a load resistor returned to ground. This ground point then becomes the virtual ground of an operational amplifier, as shown in Figs. 5 and 6. Circuit operation for the octagon circuit is briefly described as follows:

Let $X$ and $Y$ be plotted in rectangular Cartesian coordinates. With both plus and minus voltages available for each coordinate, the two diodes on either side act as sign-selection diodes to permit operation in all four quadrants. These diodes also provide additional circuit discontinuity so that the desired function can be approximated. Thus, for the resistor relationship shown, neither of the right-hand diodes conducts when $|Y/X| < 1/(1 + \sqrt{2})$, where $|Y/X|$ denotes the absolute value of the voltage ratio. Similarly, neither of the left-hand diodes conducts when $|X/Y| < 1/(1 + \sqrt{2})$. It is readily shown that the equations $|Y/X| = 1/(1 + \sqrt{2})$ and $|X/Y| = 1/(1 + \sqrt{2})$ correspond to appropriate corners of the octagon shown in Fig. A2. Note that for convenience the maximum

$$e_0 = 0.398\sqrt{X^2 + Y^2} \pm 3.96\%$$

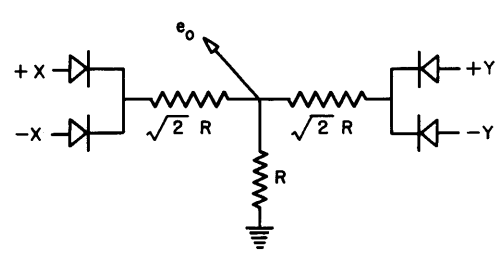


Fig. A1 - The octagon 4% function generator for $(X^2 + Y^2)^{1/2}$

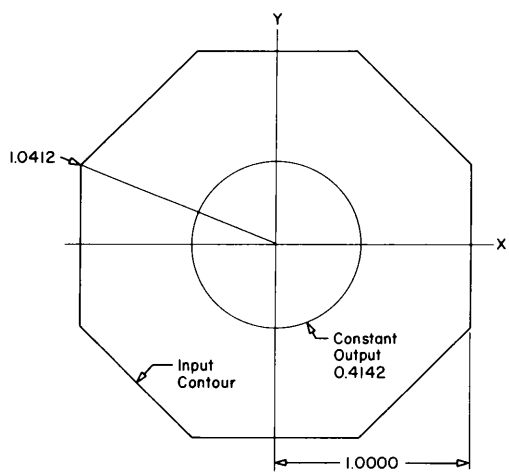


Fig. A2 - The input contour for a constant output of the 4% circuit

value of each variable is arbitrarily taken to be unity. As the input contour encloses the origin, the ratio of the two variables passes through all possible values. Thus, Fig. A2 may be thought of as representing circuit operation for all possible values of inputs $X$ and $Y$.

It can also be shown that if values of $X$ and $Y$ are constrained to follow the contour of this octagon, then the output voltage remains constant at $(\sqrt{2} - 1) = 0.4142$. Furthermore, the minimum and maximum values of $(X^2$ and $Y^2)^{1/2}$ are 1.0000 and 1.0824, respectively. These values can be used in choosing a value for the attenuation constant $K$ of Eq. (3) such that there are equal plus and minus errors $E$. Thus, Eq. (3) is more completely written as

$$e_o = K(X^2 + Y^2)^{1/2} \pm E. \qquad \text{(A1)}$$

For the above octagonal contour $K = 0.3978$ and $E = 0.01639$. For the general case where no constraints are placed on $X$ and $Y$, it is necessary to express the error in percentage form,

$$100\ E/e_o = 100(0.01639)/0.3978 = 3.96\%.$$

Thus, the low-frequency performance of the octagon circuit of Fig. A1 is described by the equation

$$e_o = 0.398(X^2 + Y^2)^{1/2} \pm 3.96\%. \qquad \text{(A2)}$$

## HIGHER ORDER POLYGONS

As discussed in Refs. A1 and A2, there are other circuits which generate the desired function with improved accuracy. These circuits require additional diodes and resistors and are characterized by regular polygons having 12, 16, 20, 24, etc. sides. For instance, it is shown in Ref. A2 how a modest increase in circuit complexity leads to a circuit characterized by a 24-sided polygon which has a theoretical accuracy of 0.4%.

## COMPENSATION FOR DIODE FORWARD POTENTIAL

The above discussion is based on the assumption that ideal diodes are used. Actual diodes introduce error; in this application with input signal swings of 10 V, the diode error is largely due to a forward potential drop of about 0.3 V. As shown in Fig. A3, this drop can be offset by introducing another potential drop equal in magnitude but opposite in polarity. Current through the additional resistors must be sufficient to keep the compensation diodes conducting at all times, with cutoff approached for a given compensation diode as the corresponding input voltage reaches its maximum positive excursion.

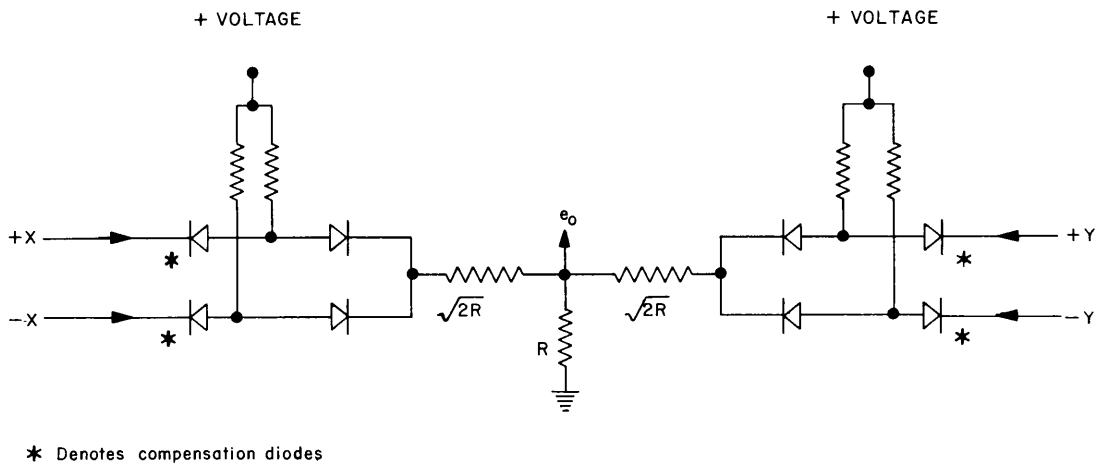


Fig. A3 - The compensation diodes for the function generator

## REFERENCES

A1. Benjamin, R., "A Simple Circuit for the Evaluation of $(X^2 + Y^2)^{1/2}$," A.S.R.E. Technical Note NX/49/1, Admiralty Signal and Radar Establishment, Great Britain, Jan. 19, 1949

\2. Benjamin, R., "Further Developments in Resistance-Diode Function Generators," A.S.R.E. Technical Note NX/49/6, Admiralty Signal and Radar Establishment, Great Britain, Mar. 2, 1949

## Appendix B

## MERIDIAN CONVERGENCE CORRECTION FACTOR

While the horizontal deflection scale factor $K_H$ is 90 naut mi/V at the equator, this must be multiplied by a dimensionless correction factor $K_\phi$ to account for meridian convergence when circle-video pulses are generated during a horizontal sweep interval corresponding to a latitude $\phi$. A formula for expressing the meridian convergence correction factor in terms of latitude will now be derived.

A parallel of latitude may be thought of as a circle formed by the intersection of the earth's spherical (assumed) surface with a plane parallel to the equatorial plane. Then the latitude $\phi$ of this intersecting plane is equal to the angle which any line from this circle through the earth's center makes with the equatorial plane, the angle being measured in the plane of the corresponding meridian. Let $R_e$ denote the radius of the spherical earth.* The circumference of any parallel of latitude is then $2\pi R_e \cos \phi$. This length varies from zero at the pole to $2\pi R_e$ at the equator, where the parallel becomes a great circle. The ratio

$$K_\phi = (2\pi R_e \cos \phi) / 2\pi R_e = \cos \phi \tag{B1}$$

evidently describes how the width (in miles) of the expanded display varies as a function of latitude, even though the width in longitude remains constant at 30 degrees. (Display height, of course, remains constant at 20 degrees or 1200 naut mi.) Thus, as the vertical off-centering varies with the display latitudes from 75 degrees south to 75 degrees north, the horizontal-sweep scale factor at latitude $\phi$ is determined by the product

$$K_H K_\phi = 90 \cos \phi \text{ naut mi/V}. \tag{B2}$$

Similarly, the scale factor for the horizontal coordinate of the circle center at latitude $\phi$ is determined by the product

$$K_R K_\phi = 255.5 \cos \phi \text{ naut mi/V}. \tag{B3}$$

Strictly speaking, the method used here to allow for meridian convergence in generating an outline of the area of view does not result in a true circle on the surface of a spherical earth. A more rigorous design approach would greatly complicate the circle circuit. Since the discrepancy is relatively minor, it will be tolerated until the requirement for a circle circuit has been established.

As explained elsewhere, $K_\phi$ is used to control the voltage gain of the $X$ amplifier when the circle circuit generates a circle on the rectangular expanded display. Then $K_\phi$ is varied in discrete steps.

---

*The symbol $R_e$ as used here is not to be confused with resistor $R_e$ of Fig. 5.

## Appendix C

## CALCULATION OF NUMERICAL VALUES FOR TABLE 1

Many of the symbols relevant to the expanded display and the associated circle circuit have numerical values used in the final design and dimensions which serve to preserve the dimensionality of the design equations. With the exception of the symbols $K$ and $K_\phi$, discussed in Appendixes A and B, respectively, the values and dimensions of these symbols are here calculated and discussed. Scale factors will be calculated first for the rectangular expanded display and then for the polar display.

For discussion purposes, gross outlines of the polar and rectangular (TV) expanded displays are shown superimposed in Fig. C1 with critical points identified by the corresponding deflection voltages. Note that, for both outlines, the horizontal and vertical raster deflection voltages are zero at the display center. For both the TV and polar rasters the horizontal raster deflection voltage is precisely adjusted to limits of -10 V at the left display extremity and +10 V at the right display extremity. Likewise, the vertical raster deflection voltage is adjusted to the same limits at the bottom and top of the two rasters.

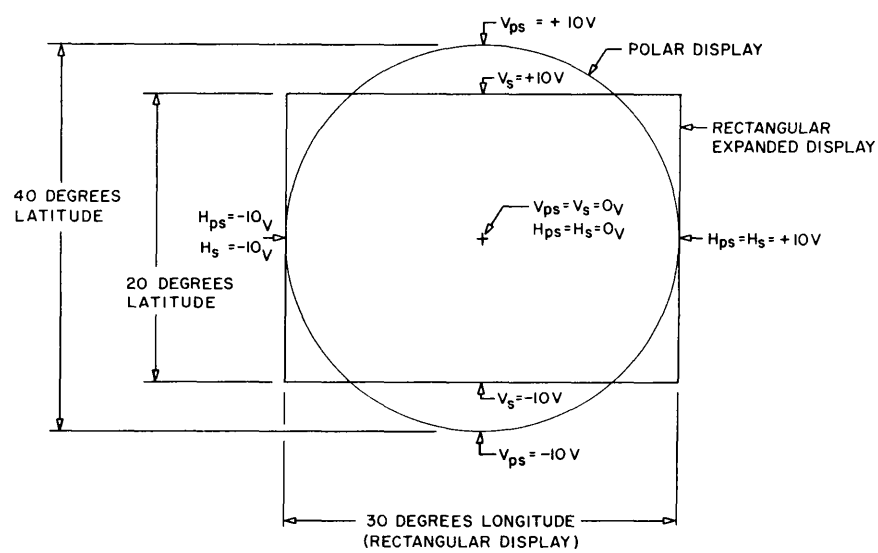


Fig. C1 - The dimensions of the two expanded displays

The circle center and circle radius voltages are generated by digital-to-analog decoders which have a zero output voltage for a zero digital input and a -10 V output for a maximum possible value of digital input signal. The least significant bit is unused in both circle-center 10-bit decoders. Since a digital count of 360 represents the right and upper extremities of both the rectangular and polar expanded displays, the maximum usable value for the vertical and horizontal circle center coordinate voltages $T_v$ and $T_h$ is $-(2\times360/1022)10$ V or -7.045 V. The digital decoders generating these voltages have an internal resistance of 6 kilohms, and this resistance forms part of the voltage mixing network.

## RECTANGULAR DISPLAY SCALE FACTORS

The associated scale factors for the circle center voltages on the rectangular expanded display are

$$K_v = (20 \text{ degrees})\,(60 \text{ naut mi/degree})/(7.045 \text{ V}) = 170.3 \text{ naut mi/V},$$

$$K_h = (30 \text{ degrees})\,(60 \text{ naut mi/degree})/(7.045 \text{ V}) = 255.5 \text{ naut mi/V}.$$

The corresponding TV raster sweep scale factors are

$$K_V = (20 \text{ degrees})\,(60 \text{ naut mi/degree})/(20 \text{ V}) = 60 \text{ naut mi/V},$$

$$K_H = (30 \text{ degrees})\,(60 \text{ naut mi/degree})/(20 \text{ V}) = 90 \text{ naut mi/V}.$$

Note that, for reasons discussed in Appendix B, the values for the two horizontal scale factors are valid only at the equator, and they must be modified by $K_\phi$ at other latitudes.

## POLAR DISPLAY SCALE FACTORS

For the circular polar display, with a radius of 20 degrees latitude, certain scale factors can be equated:

$$K_{pv} = K_{ph} = (2 \times 20 \times 60)/7.045 = 340.6 \text{ naut mi/V}$$

and

$$K_{pV} = K_{pH} = (2 \times 20 \times 60)/20 = 120 \text{ naut mi/V}.$$

Some distortion is involved, since the polar region is represented by a plane surface tangent to a spherical earth at the pole with parallels of latitude treated as equidistant circles on this plane.

## CIRCLE RADIUS SCALE FACTOR

The six-bit circle radius decoder also has an output resistance of 6 kilohms with zero output voltage representing zero radius. Since the maximum output voltage is -10 V and the least significant bit represents 8 naut mi, the circle radius scale factor is

$$K_R = 8 \text{ naut mi } (2^6 - 1)/10 \text{ V} = (8 \times 63)/10 = 50.4 \text{ naut mi/V}.$$

## Appendix D

## DESIGN PROCEDURE FOR CIRCLE GENERATOR

As stated previously, area-of-view circles are generated only for the expanded display. However, the expanded display may employ either a TV raster for the rectangular expanded display or a radial (PPI) raster depicting the polar region. While many portions of the circle generator are common to both rasters, deflection-voltage amplification must be changed with the raster. Design equations will first be derived for the TV raster used in the rectangular display. Then design equations relating $X$-axis and $Y$-axis voltage amplifications will be derived for the polar expanded display. These derivations are made with reference to the simplified block diagram of Fig. 5. Finally, the resulting design equations will be used to calculate the ohmic values shown in the circuit diagram of Fig. 6.

### DERIVATION OF DESIGN EQUATIONS FOR THE RECTANGULAR EXPANDED MODE

Let $e_y$ and $e_x$ denote the input voltages to the $Y$-axis and $X$-axis amplifiers, respectively, of Fig. 5, and assume that these amplifiers offer negligible loading at the two summing junctions. Then nodal equations for the input networks of the two amplifiers can be written as:

$$\frac{e_y - T_v}{R_3} + \frac{e_y - V_s}{R_4} + \frac{e_y - E}{R_e} = 0 \tag{D1}$$

and

$$\frac{e_x - T_h}{R_7} + \frac{e_x - H_s}{R_8} + \frac{e_x - E}{R_e} = 0 . \tag{D2}$$

Equations (D1) and (D2) are solved for their respective nodal voltages to obtain

$$e_y = \frac{R_e}{R_eR_3 + R_eR_4 + R_3R_4}\left(V_sR_3 + T_vR_4 + \frac{ER_3R_4}{R_e}\right) \tag{D3}$$

and

$$e_x = \frac{R_e}{R_eR_7 + R_eR_8 + R_7R_8}\left(H_sR_7 + T_hR_8 + \frac{ER_7R_8}{R_e}\right) . \tag{D4}$$

It will now be shown how these two nodal voltages can be interpreted in terms of distances on the earth's surface, with the further objective of deriving Eqs. (4) and (5). With correction for meridian convergence introduced according to Appendix B, information from Table 1 and Appendix C is used as follows: the instantaneous position (in nautical miles) of the sweep, measured with reference to the lower and left boundaries of the rectangular expanded display, may be expressed as

$$V = K_V(V_s + 10\,\mathrm{V})\ \text{naut mi} \tag{D5}$$

and

$$H = K_H K_\phi (H_s + 10\ \mathrm{V})\ \mathrm{naut\ mi}, \tag{D6}$$

where the constant 10 V is introduced as a boundary condition to permit $V = 0$ mi, $H = 0$ mi when $V_s = -10$ V and $H_s = -10$ V, respectively. Equations (D5) and (D6) are rearranged to obtain

$$V_s = -10 + \frac{V}{K_v}\ \mathrm{V} \tag{D7}$$

and

$$H_s = -10 + \frac{H}{K_H K_\phi}\ \mathrm{V}. \tag{D8}$$

Likewise, the circle center coordinates referenced to the lower and left boundaries, respectively, may be expressed as

$$T_v = \frac{-v}{K_v}\ \mathrm{V} \tag{D9}$$

and

$$T_h = \frac{-h}{K_h K_\phi}\ \mathrm{V}. \tag{D10}$$

Here the minus sign is introduced to permit a negative voltage to represent a positive distance.

Equations (D7) through (D10) are substituted in Eqs. (D3) and (D4), as appropriate, and the result is rearranged to obtain the amplifier input voltages

$$e_y = \frac{R_e}{R_e R_3 + R_e R_4 + R_3 R_4}\left(\frac{VR_3}{K_V} - \frac{vR_4}{K_v} + \frac{ER_3R_4}{R_e} - 10\,R_3\right) \tag{D11}$$

and

$$e_x = \frac{R_e}{R_e R_7 + R_e R_8 + R_7 R_8}\left(\frac{HR_7}{K_H K_\phi} - \frac{hR_e}{K_h K_\phi} + \frac{ER_7R_8}{R_e} - 10\,R_7\right). \tag{D12}$$

It is evident from the form of Eq. (D11) that in order for the amplifier input voltage $e_y$ to be proportional to the distance $(V - v)$, one must impose the conditions:

$$\frac{R_3}{K_V} = \frac{R_4}{K_v} \tag{D13}$$

and

$$\frac{R_4}{R_e} E = 10. \tag{D14}$$

Similarly, for the other coordinate there results the design conditions

$$\frac{R_7}{K_H} = \frac{R_8}{K_h} \tag{D15}$$

and

$$\frac{R_8}{R_e} E = 10. \tag{D16}$$

Equations (D11) and (D12) can now be written in the desired form to express the amplifier input voltages as

$$e_y = \frac{R_e R_3}{K_v (R_e R_3 + R_e R_4 + R_3 R_4)} (V - v) \text{ V} \tag{D17}$$

and

$$e_x = \frac{R_e R_7}{K_H K_\phi (R_e R_7 + R_e R_8 + R_7 R_8)} (H - h) \text{ V} . \tag{D18}$$

The corresponding output voltages of amplifiers having gains $G_y$ and $G_x$ are

$$Y = \frac{R_e R_3}{K_V (R_e R_7 + R_e R_8 + R_7 R_8)} G_y (V - v) \tag{D19}$$

and

$$X = \frac{R_e R_7}{K_H K_\phi (R_e R_3 + R_e R_4 + R_7 R_8)} G_x (H - h) . \tag{D20}$$

Equations (D19) and (D20) are Eqs. (4) and (5), respectively.

It can now be shown how the gain of the $X$ amplifier is related to that of the $Y$ amplifier.

From Table 1 and Appendix C we find that

$$K_h = 1.5 K_v , \tag{D21}$$

$$K_H = 1.5 K_V , \tag{D22}$$

and, consequently,

$$\frac{K_h}{K_H} = \frac{K_v}{K_V} . \tag{D23}$$

Furthermore, resistances $R_3$ and $R_7$ represent the 6-kilohm output resistance of the digital-to-analog decoders which provide the circle center voltages $T_v$ and $T_h$, respectively. Hence,

$$R_3 = R_7 = 6 \text{ kilohms} . \tag{D24}$$

Now, consider Eq. (D13) and use the known quantities from Appendix C to solve for $R_4$. Thus,

$$R_4 = \frac{R_3 K_v}{K_V} = 17.03 \text{ kilohms} . \tag{D25}$$

Solving Eq. (D15) for $R_8$ and using Eqs. (D23) and (D24) we can write

$$R_8 = \frac{R_7 K_h}{K_H} = \frac{R_3 K_v}{K_V} ,$$

which is clearly identical to Eq. (D25). Thus,

$$R_4 = R_8 = 17.03 \text{ kilohms} . \tag{D26}$$

Equations (D25) and (D26) can now be used to rewrite the circuit design relationship given by Eq. (6) in the simplified form

$$\frac{G_x}{K_\phi K_H} = \frac{G_y}{K_V} .$$

Solving for $G_x$ and combining with Eq. (D22) we obtain

$$G_x = 1.5 \; G_y K_\phi . \tag{D27}$$

But $K_\phi = \cos \phi$ as shown in Appendix B; thus,

$$G_x = 1.5 \; G_y \cos \phi , \tag{D28}$$

which is Eq. (15).

## DETERMINATION OF GAIN FOR THE RECTANGULAR EXPANDED MODE

Before the numerical values of $G_x$ and $G_y$ can be determined, the operating characteristics of the amplifiers must be considered. For logistical reasons the amplifiers which were primarily designed for the bootstrap sweep generators of SPAD are also used to provide the $X$ and $Y$ voltages of Fig. 5. The characteristics of this amplifier are such that the output voltage swing is limited to $\pm 10$ V; the gain of the amplifiers should be restricted to a minimum of $+2$, and the load resistance should not be less than 200 ohms or greater than 1000 ohms.

With the foregoing amplifier operating conditions the gain values can now be determined. In the interval from 79°56'40" to 78°46'40", where the gain of the $X$ amplifier should be a minimum, it can be seen in Table F1 that $\cos \phi$ was chosen to be 0.18406. Thus, let

$$G_x(\text{min}) = +2 \tag{D29}$$

when $\cos \phi = 0.18406$. It is now possible to determine $G_y$ from Eq. (D28) as follows:

$$G_x(\text{min}) = 1.5 \times 0.18406 \times G_y = +2 ,$$

and

$$G_y = 2/(1.5 \times 0.18406) = 7.244 . \tag{D30}$$

Since there is no latitudinal distortion of the subsatellite circle, this value of the $Y$ amplifier gain remains constant over the entire rectangular expanded mode. The amplifier configurations used to implement these gains are discussed in Appendix E.

Before we proceed to calculate the offset current $E/R_e$, it is necessary to introduce another boundary condition. A maximum radius of 500 naut mi for the subsatellite circle was tentatively specified in Ref. 1. Using digital circuits and a circle-radius data word composed of six binary bits, with the least significant bit weighted at 8 naut mi, it was convenient to generate a circle having a maximum radius of $(2^6 - 1)8 = 504$ naut mi. Now, when the circle radius is a maximum at the equator, the amplifiers should deliver their maximum voltage. Hence, when $(V - v) = \pm 504$ naut mi, $Y = \pm 10$ V. If we now consider Eq. (D19) and impose the foregoing condition, we have

$$Y = \frac{R_e R_3 G_y}{K_v(R_e R_3 + R_e R_4 + R_3 R_4)} (V - v) = 10 \text{ V}$$

whenever $(V - v)$ = 504 naut mi. Solving for $R_e$ we obtain

$$R_e = \frac{10 K_V R_3 R_4}{R_3 G_y (V - v) - 10 K_V (R_3 R_4)} . \tag{D31}$$

Substituting the known values, we calculate

$$R_e = 7.580 \text{ kilohms} .$$

Finally, from Eq. (D14) we find the offset voltage $E$ to be

$$E = \frac{10 R_e}{R_4} = 4.451 \text{ V} .$$

For convenience (see Fig. 6) the quantities $E$ and $R_e$ were obtained somewhat indirectly using both a positive and a negative supply of 30 V and resistors $R_{14}$, $R_{15}$, $R_{16}$, and $R_{17}$ for the $Y$ input network, and $R_{18}$, $R_{19}$, $R_{20}$, and $R_{39}$ for the $X$ input network. The 500-ohm potentiometer in the center of a voltage-divider chain provides a voltage $E$ adjustable from 3.5 V to 5.5 V with negligible variation in the equivalent source resistance of this voltage.

## OHMIC VALUES FOR RESISTOR-DIODE FUNCTION GENERATOR

As mentioned previously, resistor $R_{11}$ of Fig. 5 is actually an integral part of the function generator even though it is drawn external to the block. In the more detailed schematic of Fig. 6 the resistor-diode function generator is seen to be composed of resistors $R_9$, $R_{10}$, and $R_{11}$, and the associated diode network. Ohmic values for these resistors can now be determined. Equation (14) is solved for $R_{11}$ to obtain

$$R_{11} = \frac{K K_R R_e R_3 R_{12} G_y}{K_V (R_e R_3 + R_e R_4 + R_3 R_4)} . \tag{D32}$$

Substituting the known values from Appendixes A and C and values of the components determined in this appendix, $R_{11}$ is found to be

$$R_{11} = 2.388 \text{ kilohms} .$$

Furthermore, it is stated in Appendix A that the resistor ratio for the octagon generator is

$$\frac{R_9}{R_{11}} = \frac{R_{10}}{R_{11}} = \sqrt{2} . \tag{D33}$$

From this it follows that

$$R_9 = R_{10} = \sqrt{2}\, R_{11} = 3.376 \text{ kilohms} .$$

The inevitable forward voltage drops of the sign-selection diodes are partially compensated for by resistors $R_{32}$, $R_{33}$, $R_{34}$, and $R_{35}$ and diodes $D_1$, $D_2$, $D_5$, and $D_6$, as shown in Fig. 6.

## DERIVATION OF THE DESIGN EQUATIONS FOR THE POLAR EXPANDED MODE

An abbreviated development can be considered for the polar mode, since we shall follow the approach used for the rectangular mode, subject to the conditions mentioned in the text. The subscript $p$ will designate the polar mode counterparts to the rectangular mode. Thus, $e_{px}$ and $e_{py}$ denote the inputs to the $X$ and $Y$ amplifiers, respectively, of Fig. 5 during the polar mode of operation.

By inspection, Eqs. (D3) and (D4) can be written for the polar case as

$$e_{py} = \frac{R_e}{R_e R_{p3} + R_e R_{p4} + R_{p3} R_{p4}} \left( V_{ps} R_{p3} + T_v R_{p4} + \frac{E R_{p3} R_{p4}}{R_e} \right) \tag{D34}$$

and

$$e_{px} = \frac{R_e}{R_e R_{p7} + R_e R_{p8} + R_{p7} R_{p8}} \left( H_{ps} R_{p7} + T_h R_{p8} + \frac{E R_{p7} R_{p8}}{R_e} \right) . \tag{D35}$$

Substituting the appropriate quantities from Table 1 and Appendix C, these equations become

$$e_{py} = \frac{R_e R_{p3}}{K_{pV} ( R_e R_{p3} + R_e R_{p4} + R_{p3} R_{p4} )} \; (V - v) \tag{D36}$$

and

$$e_{px} = \frac{R_e R_{p7}}{K_{pH} ( R_e R_{p7} + R_e R_{p8} + R_{p7} R_{p8} )} \; (H - h) , \tag{D37}$$

provided

$$R_{p3}/K_{pV} = R_{p4}/K_{pv} , \tag{D38}$$

$$R_{p7}/K_{pH} = R_{p8}/K_{ph} , \tag{D39}$$

$$E R_{p4}/R_e = 10 , \tag{D40}$$

and

$$E R_{p7}/R_e = 10 . \tag{D41}$$

A happy consequence of generating precision sweep and circle center voltages is that the bias voltage $E$ and the associated resistor $R_e$ need not be changed for the polar display.

The amplifier output voltages are then

$$Y_p = \frac{R_e R_{p3} G_{py}}{K_{pV} ( R_e R_{p3} + R_e R_{p4} + R_{p3} R_{p4} )} \; (V - v) \tag{D42}$$

and

$$X_p = \frac{R_e R_{p7} G_{px}}{K_{pH} ( R_e R_{p7} + R_e R_{p8} + R_{p7} R_{p8} )} \; (H - h) , \tag{D43}$$

where $G_{py}$ and $G_{px}$ are the gains of the $Y$ and $X$ amplifiers during polar operation. Note that the meridian convergence correction factor $K_\phi$ has been omitted from the polar equations.

From Appendix F we can derive the relationships

$$\frac{K_h}{K_H} = \frac{K_v}{K_V} = \frac{K_{pv}}{K_{pV}} = \frac{K_{ph}}{K_{pH}} \ . \tag{D44}$$

Since $R_{p3}$ and $R_{p7}$ are the output resistances of the $D/A$ decoders, it follows that $R_{p3} = R_3$ and $R_{p7} = R_7$. We can now solve for $R_{p4}$ and $R_{p8}$, using Eqs. (D44) and (D25) as follows:

$$R_{p4} = \frac{R_{p3}K_{pv}}{K_{pV}} = \frac{R_3 K_v}{K_V} = R_4 \tag{D45}$$

and

$$R_{p8} = \frac{R_{p7}K_{ph}}{K_{pH}} = \frac{R_7 K_h}{K_H} = R_8 \ . \tag{D46}$$

Furthermore, since from Eq. (D26) $R_4 = R_8$, it is evident that the input networks composed of resistors $R_3$, $R_4$, and $R_e$ for the $X$ amplifier and $R_7$, $R_8$, and $R_e$ for the $Y$ amplifier are identical for both the polar and rectangular expanded modes. Thus the same network can be used for both modes without any circuit element switching, provided the rectangular and the polar sweeps are accurately calibrated.

Now, to determine the gain relationships required we can substitute Eqs. (D42) and (D43) into Eq. (3), equate the coefficients of $(V - v)$ and $(H - h)$ and use the above resistor equalities to obtain the polar design relationship

$$\frac{R_7 R_e G_{px}}{K_{pH}(R_e R_7 + R_e R_8 + R_7 R_8)} = \frac{R_3 R_e G_{py}}{K_{pV}(R_e R_3 + R_e R_4 + R_3 R_4)} \ . \tag{D47}$$

The equation for voltage $e_{po}$ at the output of the function generator can now be written as

$$e_{po} = \frac{K R_e R_3 G_{py}}{K_{pV}(R_e R_3 + R_e R_4 + R_3 R_4)} \left[(H-h)^2 + (V-v)^2\right]^{1/2} \tag{D48}$$

Substituting $R_7 = R_3$, $R_8 = R_4$, and the relation

$$K_{pH} = K_{pV} \tag{D49}$$

obtained from Appendix C, Eq. (D47) reduces to

$$G_{px} = G_{py} \ . \tag{D50}$$

With the comparator circuit already designed for the rectangular mode and the component values determined by the appropriate scale factors of that mode, it was desirable to complete the polar mode design using the same comparator circuit, thus eliminating the need for additional circuit-element switching. It also appeared useful to express the value of the polar gain in terms of the previously determined rectangular gain. This is done by letting the output voltage $e_o$ for the rectangular mode equal $e_{po}$, the corresponding voltage for the polar mode. Thus, Eqs. (7) and (D48) are combined and simplified to obtain

$$\frac{G_y}{K_V} = \frac{G_{py}}{K_{pV}} \ . \tag{D51}$$

But from Appendix C we find that

$$2K_V = K_{pV} .$$

Thus, Eq. (D51) above reduces to

$$G_{py} = 2G_y . \tag{D52}$$

This result is combined with Eq. (D50) to obtain

$$G_{py} = G_{px} = 2G_y , \tag{D53}$$

which is Eq. (16).

## Appendix E

## DIGITAL CONTROL OF AMPLIFIER GAIN

The design equations for digital control of the gain of a noninverting voltage amplifier with negative feedback are derived here. Ohmic values are also calculated for the circuit of Fig. 6.

### DERIVATION OF DESIGN EQUATIONS

A noninverting voltage amplifier with negative feedback commonly has the configuration shown in Fig. E1, where a high-gain differential operational amplifier employs resistors $R_s$ and $R_g$ to provide negative feedback such that the voltage amplification is approximated by the equation

$$G = \frac{e_o}{e_i} \approx 1 + \frac{R_s}{R_g} . \tag{E1}$$

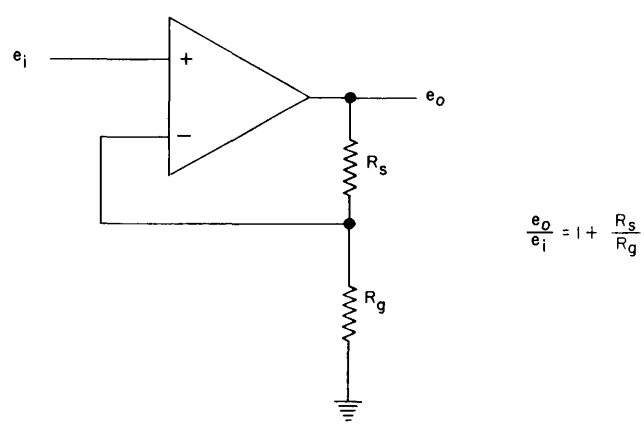


Fig. E1 - The positive-gain amplifier

It is assumed that the amplifier input offers negligible loading effect on the feedback network.

The voltage amplification can be altered by replacing one or more of the resistors. As an alternative, a calibrated, manually adjusted variable resistor is sometimes used to vary the amplification.

However, when the amplification must be more rapidly varied and the advantages of negative feedback retained, the circuit of Fig. E1 can be augmented by selectively switching the resistors $R_{f0}$, $R_{f1}$, $R_{f2}$, . . . , $R_{fn}$ in parallel with the fixed resistor $R_g$ thereby varying the overall amplification in discrete increments. For convenience, one end of

each of these resistors is tied to the junction of $R_g$ and $R_s$, and the switching is accomplished by using switches $S_0$, $S_1$, $S_2$, ..., $S_n$, as shown in Fig. E2. While manually operated mechanical switches can be used, digitally controlled bidirectional clamps can also be used to vary the amplification with a transition time of about a microsecond.

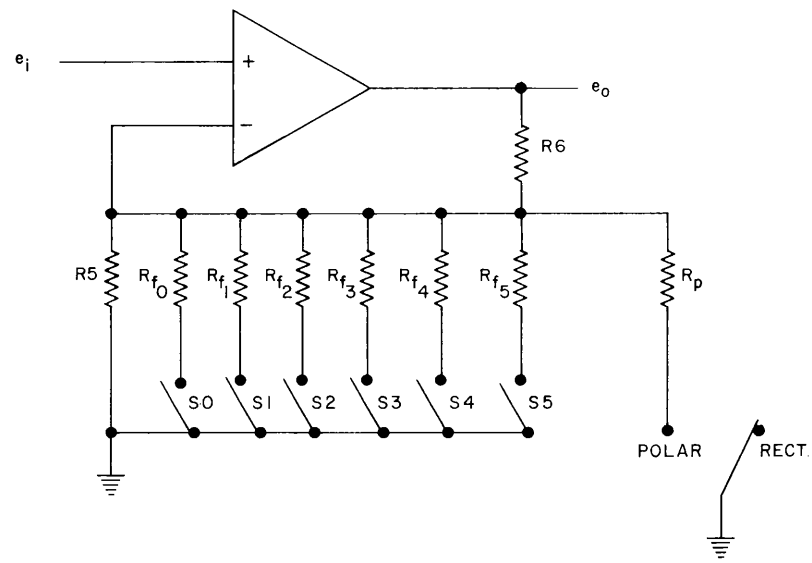


$$\text{RECTANGULAR GAIN} = \frac{e_o}{e_i} = 1 + \frac{R6}{R5} + \sum_{j=0}^{5} \frac{R6}{R_{f_j}} S_j$$

$$\text{POLAR GAIN} = \frac{e_o}{e_i} = 1 + \frac{R6}{R5} + \frac{R6}{R_p}$$

Fig. E2 - The $X$ amplifier

An equation can be used to represent the voltage amplification of the circuit in Fig. E2. Let $S_j$ designate a weighting coefficient which is either zero or one. When switch $S_j$ is closed, $S_j = 1$; when switch $S_j$ is open, $S_j = 0$. Now $j = 0, 1, 2, \ldots, n$, and as before $n$ is a positive integer. Then for Fig. E2,

$$G = 1 + \frac{R_s}{R_g} + \sum_{j=0}^{n} \frac{R_s}{R_{fj}} S_j \,. \tag{E2}$$

Equation (E2) may be interpreted physically as quantizing the effect of adding one or more of the resistors $R_{fj}$ in parallel with $R_g$.

While the switched resistors $R_{f1}$ through $R_{fn}$ can bear any arbitrary relation to the switched resistor $R_0$, it is convenient to assign the relation

$$R_{fj} = 2^{-j} R_{f0}, \quad j = 1, 2, \ldots, n \,. \tag{E3}$$

By substitution, Eq. (E2) then becomes

$$G = 1 + \frac{R_s}{R_g} + \frac{R_s}{R_{f0}} \sum_{j=0}^{n} 2^j S_j \,. \tag{E4}$$

The expression

$$\sum_{j=0}^{n} 2^j S_j$$

represents a binary number of $(n+1)$ bits denoting any desired integral value from zero to $(2^{n+1} - 1)$. Thus, the voltage amplification could then be varied in discrete, uniform steps

$$\Delta G = \frac{R_s}{R_{f0}} , \tag{E5}$$

from the minimum value

$$G(\min) = 1 + \frac{R_s}{R_g} \tag{E6}$$

to the maximum value

$$G(\max) = G(\min) + \Delta G(2^{n+1} - 1) . \tag{E7}$$

## CALCULATION OF OHMIC VALUES

From Eq. (E6) it is evident that the minimum gain occurs when all the switches are open; i.e., $S_0, \ldots, S_5 = 0$. Similarly, from Eq. (E7), the maximum gain occurs when all the switches are closed; i.e., $S_0, \ldots, S_5 = 1$. First consider the case of minimum gain. Then

$$G_x = 1 + \frac{R_s}{R_g} = +2 ,$$

and

$$R_s = R_g .$$

In Fig. E2 $R_s$ and $R_g$ correspond to $R_6$ and $R_5$, respectively. Now, recalling that the maximum resistance to be driven by the amplifiers was fixed at 1000 ohms, let

$$R_5 + R_6 = 1000 \text{ ohms} .$$

Then

$$R_5 = R_6 = 0.5 \text{ kiloms} .$$

Using the values for $\cos\phi$ from Table F1 and the value for $G_y$ of 7.244, Eq. (D28) was solved for the 32 discrete values of $G_x$. These values are shown in Table E1 under the heading "Computed Gain," where this gain is obtained from the relation

$$\text{computed gain } G_x = 10.866 \cos\phi . \tag{E8}$$

In Eq. (E4) if we let $n = 5$ (that is, provide for six switchable resistors), then 64 discrete values of the gain can be obtained. With $\Delta G$ equal to 0.141, 32 of the 64 possible values were found which suitably matched the computed gain values. The values so obtained are shown in Table E1 under the heading "Obtained Gain," where this gain is given by

Table E1
Horizontal Gains for Meridian Convergence

| OD Gate | Computed* Gain | Obtained† Gain | $\Sigma S_j 2^j$ | $j$ For $S_j = 1$ |
|---|---|---|---|---|
| 1-0 | 2.00 | 2.00 | 0 | — |
| 1-1 | 2.23 | 2.28 | 2 | 1 |
| 1-2 | 2.47 | 2.42 | 3 | 1, 0 |
| 1-3 | 2.70 | 2.71 | 5 | 2, 0 |
| 1-4 | 2.93 | 2.98 | 7 | 2, 1, 0 |
| 1-5 | 3.15 | 3.13 | 8 | 3 |
| 1-6 | 3.38 | 3.41 | 10 | 3, 1 |
| 1-7 | 3.60 | 3.55 | 11 | 3, 1, 0 |
| 2-0 | 3.83 | 3.83 | 13 | 3, 2, 0 |
| 2-1 | 4.05 | 4.11 | 15 | 3, 2, 1, 0 |
| 2-2 | 4.27 | 4.26 | 16 | 4 |
| 2-3 | 4.49 | 4.54 | 18 | 4, 1 |
| 2-4 | 4.70 | 4.68 | 19 | 4, 1, 0 |
| 2-5 | 4.91 | 4.96 | 21 | 4, 2, 0 |
| 2-6 | 5.13 | 5.10 | 22 | 4, 2, 1 |
| 2-7 | 5.33 | 5.38 | 24 | 4, 3 |
| 3-0 | 5.63 | 5.67 | 26 | 4, 3, 1 |
| 3-1 | 6.03 | 6.09 | 29 | 4, 3, 2, 0 |
| 3-2 | 6.42 | 6.37 | 31 | 4, 3, 2, 1, 0 |
| 3-3 | 6.80 | 6.79 | 34 | 5, 1 |
| 3-4 | 7.16 | 7.22 | 37 | 5, 2, 0 |
| 3-5 | 7.51 | 7.50 | 39 | 5, 2, 1, 0 |
| 3-6 | 7.85 | 7.80 | 41 | 5, 3, 0 |
| 3-7 | 8.16 | 8.20 | 44 | 5, 3, 2 |
| 4-0 | 8.60 | 8.63 | 47 | 5, 3, 2, 1, 0 |
| 4-1 | 9.15 | 9.19 | 51 | 5, 4, 1, 0 |
| 4-2 | 9.63 | 9.61 | 54 | 5, 4, 2, 1 |
| 4-3 | 10.03 | 10.03 | 57 | 5, 4, 3, 0 |
| 4-4 | 10.35 | 10.32 | 59 | 5, 4, 3, 1, 0 |
| 4-5 | 10.60 | 10.60 | 61 | 5, 4, 3, 2, 0 |
| 4-6 | 10.76 | 10.74 | 62 | 5, 4, 3, 2, 1 |
| 4-7 | 10.85 | 10.88 | 63 | 5, 4, 3, 2, 1, 0 |

*Computed gain = $10.866 \cos \phi$.

†Obtained gain $= 2 + \Delta G \sum_{j=0}^{n} S_j 2^j = 2 + 0.141 \sum_{j=0}^{5} S_j 2^j$ .

$$\text{obtained gain } G_x = 1 + \frac{R_6}{R_s} + \Delta G \sum_{j=0}^{5} S_j 2^j$$

$$= 2 + 0.141 \sum_{j=0}^{5} S_j 2^j \ . \tag{E9}$$

The fourth column of Table E1 lists the multiples of $\Delta G$ required to obtain the gains shown. The last column indicates which resistor or combination of resistors must be switched into the circuit to provide the values shown in the fourth column. The numbers here were subsequently used to designate which of the BDC units are activated, as shown in Table 1.

We now calculate the six resistor values $R_{fj}$, where $j = 0, \ldots, 5$. Equation (E5) can readily be solved for $R_{f0}$:

$$R_{f0} = \frac{R_s}{\Delta G} = \frac{0.5k}{0.141} = 3.546 \text{ kilohms} .$$

Equation (E3) can now be solved for the remaining resistors as follows:

$$R_{f1} = 2^{-1}R_{f0} = 2^{-1}(3.546k) = 1.773 \text{ kilohms} ,$$

$$R_{f2} = 2^{-2}R_{f0} = 2^{-2}(3.546k) = 0.8865 \text{ kilohms} ,$$

$$R_{f3} = 2^{-3}R_{f0} = 2^{-3}(3.546k) = 0.4433 \text{ kilohms} ,$$

$$R_{f4} = 2^{-4}R_{f0} = 2^{-4}(3.546k) = 0.2216 \text{ kilohms} ,$$

and

$$R_{f5} = 2^{-5}R_{f0} = 2^{-5}(3.546k) = 0.1082 \text{ kilohms} .$$

Note that $R_{f0}$ through $R_{f5}$ correspond to $R_{26}$ through $R_{21}$ of Fig. 6, respectively. This completes the design of the $X$ coordinate circuitry for the rectangular expanded display.

The $Y$ amplifier configuration shown in Fig. E3 was established by a few practical considerations. To keep lead runs from the output to the input of the amplifiers as short as possible, all feedback resistors were placed on the same plug-in module as the differential amplifier. Furthermore, it was decided that the $X$ and $Y$ amplifier modules should be interchangeable.

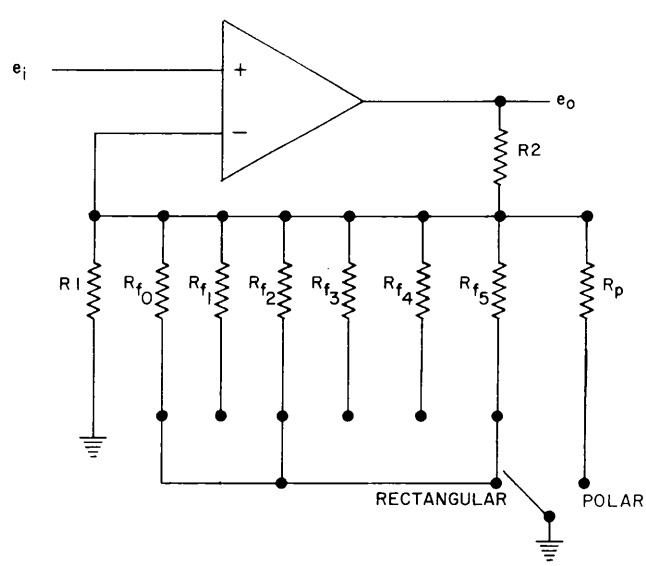


$$\text{RECTANGULAR GAIN} = \frac{e_o}{e_i} = 1 + \frac{R2}{R1} + R2\left(\frac{1}{R_{f0}} + \frac{1}{R_{f2}} + \frac{1}{R_{f5}}\right)$$

$$\text{POLAR GAIN} = \frac{e_o}{e_i} = 1 + \frac{R2}{R1} + \frac{R2}{R_p}$$

Fig. E3 - The $Y$ amplifier

It will be recalled that the gain of the $Y$ amplifier $G_y$ was determined to be 7.244 and that this value remains constant for the rectangular expanded mode of operation. Evidently no switching of feedback resistors is required. Table E1 shows that a gain of 7.22 is obtained when the binary exponent $j$ is 5, 2, and 0, i.e., when resistors $R_{f5}$, $R_{f2}$, and $R_{f0}$ are in the feedback loop. Thus, by connecting these three resistors and tying them to ground we can obtain the desired gain within a fraction of a percent. Resistors $R_{f0}$, $R_{f2}$, and $R_{f5}$ of Fig. E3 correspond to resistors $R_{30}$, $R_{29}$, and $R_{28}$, respectively, of Fig. 6.

Finally, we can determine the configuration necessary to implement the gains $G_{px}$ and $G_{py}$ for the polar mode. From Eq. (E1) we can write the equation for the gain of the amplifier in Fig. E1 as

$$G = 2 \times 7.244 = 14.488 = 1 + \frac{R_s}{R_g} . \tag{E10}$$

Since the gains of both the $X$ and $Y$ amplifiers during polar mode are equal (see Eq. (D50)), we will consider only the $X$ amplifier of Fig. E2. In this configuration $R_s$ of Eq. (E10) corresponds to $R_6$, and $R_g$ is the parallel combination of resistors $R_5$ and $R_p$. Equation (E10) can now be rewritten as

$$1 + \frac{R_6}{R_5} + \frac{R_6}{R_p} = 14.488 .$$

Substituting values of 0.5 kilohms for both $R_5$ and $R_6$, we can solve for $R_p$ to set $R_p$ = 40 ohms.

## Appendix F

## STEPWISE APPROXIMATION TO MERIDIAN CONVERGENCE CONTOUR

In Appendix B it is shown that to compensate for meridian convergence on the rectangular expanded display, the correction factor $K_\phi = \cos\phi$ is used to control the gain of the longitudinal or $X$ amplifier as a function of latitude $\phi$. To limit the circuitry to a reasonable size and yet maintain an overall accuracy consistent with an octagonal approximation to a circle, the cosine function is approximated by 32 discrete values for the latitude interval within 80 degrees of the equator. The maximum error introduced is 5.4% in the interval 78°46'40" to 79°56'40" and not more than 0.17% in the interval 0°3'20" to 4°56'40". Further figures are shown in Table F1. The apparent odd limits of each interval are due to dividing the intervals into a discrete number of raster lines with each line corresponding to an increment of 3'20" of latitude. Thus, from 80° to 60°, the intervals contain 23 raster lines (1°13'); from 60° to 40° the intervals contain 45 raster lines (2°26'); and from 40° to 0°, the intervals contain 90 raster lines (4°53').

Table F1
Data for Stepwise Approximation to Cosine Function

| OD Gate | Latitude Interval | $\cos\phi$ | Percent Error |
|---|---|---|---|
| 1-0 | 79°56'40" - 78°46'40" | 0.18406 | 5.41 |
| 1-1 | 78°43'20" - 77°30' | 0.20547 | 5.07 |
| 1-2 | 77°26'40" - 76°13'20" | 0.22729 | 4.56 |
| 1-3 | 76°10' - 75°3'20" | 0.24814 | 3.78 |
| 1-4 | 74°56'40" - 73°46'40" | 0.26920 | 3.64 |
| 1-5 | 73°43'20" - 72°30' | 0.29015 | 3.51 |
| 1-6 | 72°26'40" - 71°13'20" | 0.31143 | 3.25 |
| 1-7 | 71°10' - 70°3'20" | 0.33171 | 2.75 |
| 2-0 | 69°56'40" - 68°46'40" | 0.35220 | 2.70 |
| 2-1 | 68°43'20" - 67°30' | 0.37253 | 2.65 |
| 2-2 | 67°26'40" - 66°13'20" | 0.39314 | 2.49 |
| 2-3 | 66°10' - 65°3'20" | 0.41273 | 2.14 |
| 2-4 | 64°56'40" - 63°46'40" | 0.43251 | 2.12 |
| 2-5 | 63°43'20" - 62°30' | 0.45202 | 2.10 |
| 2-6 | 62°26'40" - 61°13'20" | 0.47181 | 1.99 |
| 2-7 | 61°10' - 60°3'20" | 0.49056 | 1.72 |
| 3-0 | 59°56'40" - 57°30' | 0.51844 | 3.51 |
| 3-1 | 57°26'40" - 55°3'20" | 0.55490 | 3.12 |
| 3-2 | 54°56'40" - 52°30' | 0.59105 | 2.90 |
| 3-3 | 52°26'40" - 50°3'20" | 0.62534 | 2.59 |
| 3-4 | 49°56'40" - 47°30' | 0.65919 | 2.42 |
| 3-5 | 47°26'40" - 45°3'20" | 0.69102 | 2.17 |
| 3-6 | 44°56'40" - 42°30' | 0.72223 | 2.03 |
| 3-7 | 42°26'40" - 40°3'20" | 0.75138 | 1.83 |
| 4-0 | 39°56'40" - 35°3'20" | 0.79177 | 3.27 |
| 4-1 | 34°56'40" - 30°3'20" | 0.84202 | 2.71 |
| 4-2 | 29°56'40" - 25°3'20" | 0.88576 | 2.22 |
| 4-3 | 24°56'40" - 20°3'20" | 0.92277 | 1.76 |
| 4-4 | 19°56'40" - 15°3'20" | 0.95269 | 1.34 |
| 4-5 | 14°56'40" - 10°3'20" | 0.97531 | 0.94 |
| 4-6 | 9°56'40" - 5°3'20" | 0.99051 | 0.56 |
| 4-7 | 4°56'40" - 0°3'20" | 0.99816 | 0.17 |

The value of the cosine chosen for each interval is such that equal errors are caused by the deviation of the function from this value at either limit of the interval. Hence, the percent error shown in Table F1 is the maximum error which can be expected within the corresponding interval. Obviously, somewhere near the midpoint of each interval the error passes through zero. This is evident from Fig. F1, which compares the cosine function with its stepwise approximation.

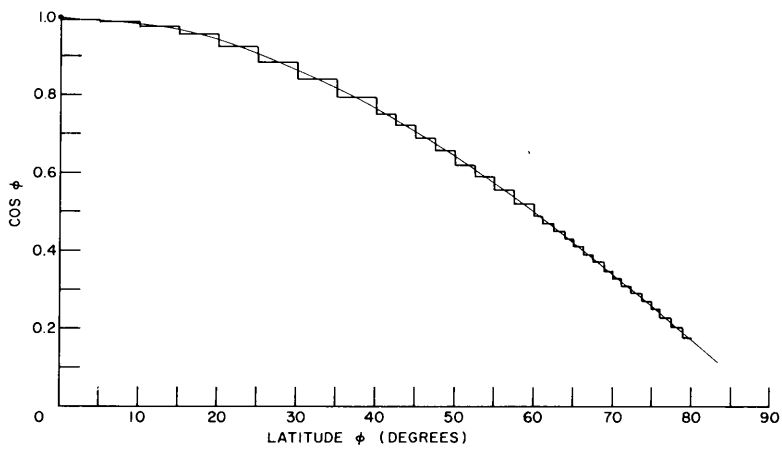


Fig. F1 - The stepwise approximation of the cosine function

Security Classification

**DOCUMENT CONTROL DATA - R & D**

*(Security classification of title, body of abstract and indexing annotation must be entered when the overall report is classified)*

| | |
|---|---|
| 1. ORIGINATING ACTIVITY *(Corporate author)*<br>Naval Research Laboratory<br>Washington, D.C. 20390 | 2a. REPORT SECURITY CLASSIFICATION<br>Unclassified<br>2b. GROUP |

3. REPORT TITLE

A SUBSATELLITE AREA-OF-VIEW CIRCUIT

4. DESCRIPTIVE NOTES *(Type of report and inclusive dates)*
This is an interim report; work on the problem continues.

5. AUTHOR(S) *(First name, middle initial, last name)*

R.J. Orsino and H.G. Talmadge, Jr.

| | | |
|---|---|---|
| 6. REPORT DATE<br>April 30, 1968 | 7a. TOTAL NO. OF PAGES<br>42 | 7b. NO. OF REFS<br>10 |
| 8a. CONTRACT OR GRANT NO.<br>NRL Problem Y01-01<br>b. PROJECT NO.<br>XF 019-01-03-6168<br>c.<br>d. | 9a. ORIGINATOR'S REPORT NUMBER(S)<br>NRL Report 6660<br>9b. OTHER REPORT NO(S) *(Any other numbers that may be assigned this report)* | |

10. DISTRIBUTION STATEMENT

This document has been approved for public release and sale; its distribution is unlimited.

| | |
|---|---|
| 11. SUPPLEMENTARY NOTES | 12. SPONSORING MILITARY ACTIVITY<br>Department of the Navy (Naval Ship Systems Command), Washington, D.C. 20360 |

13. ABSTRACT

A subsatellite circle circuit is included in the NRL experimental satellite position prediction and display equipment (SPAD). The circuit paints, on the expanded display, a circle enclosing the area of view for a selected satellite. A combination of digital and analog techniques is used to generate a polygonal approximation to the ideal circle. Compensation for meridian convergence is provided, so that the resulting error is roughly equal to the degree to which an octagon approximates a circle. With simple circuit changes the polygon could have 12, 16, 20, or more sides.

The circle center is defined by the subsatellite position, and the SPAD prediction computer uses the satellite look-cone angle (say, that of a cloud-cover camera) and the satellite height to generate a circle radius in increments of 8 naut mi up to a maximum radius of 504 naut mi. This limit is determined by the practical requirement of displaying the circle only on the expanded display of limited area for any portion of the earth's surface. A duplicate circuit generates a circle about own ship's position.

(over)

DD FORM 1 NOV 65 1473 (PAGE 1)

S/N 0101-807-6801



Security Classification

Security Classification

| 14. KEY WORDS | LINK A ROLE | LINK A WT | LINK B ROLE | LINK B WT | LINK C ROLE | LINK C WT |
|---|---|---|---|---|---|---|
| Subsatellite circle circuit | | | | | | |
| Satellite position prediction and display (SPAD) | | | | | | |
| Display systems | | | | | | |
| Polar display | | | | | | |
| Rectangular display | | | | | | |
| Shipborne | | | | | | |

The operational significance to be attached to the circles is of no concern in the present study. Rather, the circuit design approach, the design equations, and circuit description at the block-diagram level are the important elements.

With suitable modification the circle circuit used for SPAD is applicable to any cathode-ray tube display having either electrostatic or magnetic deflection, providing the entire display surface is scanned by a method involving two orthogonal axes of deflection. The application is quite general and is not limited to the SPAD display of the earth's surface.